

This is an Open Access document downloaded from ORCA, Cardiff University's institutional repository: <https://orca.cardiff.ac.uk/id/eprint/146128/>

This is the author's version of a work that was submitted to / accepted for publication.

Citation for final published version:

Cerasale, Daniel J., Ward, Dominic C. and Easun, Timothy L. 2022. MOFs in the time domain. *Nature Reviews Chemistry* 6 , pp. 9-30. 10.1038/s41570-021-00336-8

Publishers page: <http://dx.doi.org/10.1038/s41570-021-00336-8>

Please note:

Changes made as a result of publishing processes such as copy-editing, formatting and page numbers may not be reflected in this version. For the definitive version of this publication, please refer to the published source. You are advised to consult the publisher's version if you wish to cite this paper.

This version is being made available in accordance with publisher policies. See <http://orca.cf.ac.uk/policies.html> for usage policies. Copyright and moral rights for publications made available in ORCA are retained by the copyright holders.



MOFs in the Time Domain

Daniel J. Cerasale, Dominic C. Ward and Timothy L. Easun*
School of Chemistry, Cardiff University, Main Building, Park Place, Cardiff CF10 3AT, UK

Abstract

Many of the proposed applications of metal-organic framework (MOF) materials may fail to materialise if the community doesn't fully address the difficult fundamental work needed to map out the time-gap in the literature. While there are a range of excellent investigations into MOF dynamics and time-dependent phenomena, generally these works represent only a tiny fraction of the vast field of MOF studies. This review provides an overview of current research into the temporal evolution of MOF structures and properties by analysis of the time-resolved experimental techniques that can be used to monitor such behaviours. We focus on new and innovative techniques, while also discussing older methods well-utilised with other chemical systems. Four areas are examined: MOF formation, guest motion, electron motion, and framework motion. In each area, we highlight the disparity between the relatively small amount of (published) research on key time-dependent phenomena and the enormous scope for acquiring wider and deeper understanding essential for the future of the field.

Introduction

New metal-organic frameworks (MOFs) are frequently being added to the literature, but the days of simply reporting just a static, pretty MOF structure are largely behind us. The most exciting studies of the present day are those describing the time-dependent phenomena which more accurately represent the real state of any given MOF crystal or particle and of the guests within. Detailed new investigations into fundamentally dynamic phenomena in chemistry and physics such as nanofluidics,¹ ion or electron conduction^{2,3} and photochemistry^{4,5} have been enabled by the highly crystalline nature of the majority of MOFs, studied with techniques such as X-ray/neutron diffraction,^{6,7} spectroscopy⁸ and microscopy methods.⁹ Since linker size/shape/property variation is limited only by the ingenuity of synthetic chemists, and many different metal ions can be combined with the resulting linkers, the accessible dynamic chemical phase space afforded by MOFs is vast.¹⁰⁻¹³

The high degree of intrinsic structural variation gives rise to one of the most appealing features of MOFs: extremely high tunability of framework properties such as pore size, shape, surface area and chemistry. This, in turn, allows for their targeted use in a variety of applications including gas storage and separation,¹⁴⁻¹⁶ photocatalysis,^{17,18} drug delivery,¹⁹⁻²² sensing²³⁻²⁵ and fuel cells.^{26,27}

The term "soft porous crystals" (SPCs) coined in 2009 by Kitagawa and co-workers²⁸ describes a subclass of MOF which display some degree of framework flexibility while maintaining structural integrity throughout reversible framework changes caused by stimuli including temperature,²⁹ pressure,³⁰ guest variation³¹ or light.³² These "flexible" MOFs may appear to be considerably less abundant in crystal structure databases than their rigid counterparts, but it is also likely that the flexibility limits of most reported frameworks have simply not been investigated.³³

Understanding the fundamental physics and chemistry governing the mechanisms of structural transformations in flexible frameworks is key to successful development of applications. Quantum chemistry calculations and molecular dynamics/grand canonical Monte Carlo simulation (MD/GCMC)

can provide some mechanistic insight^{34,35} but are often limited to largely idealised and spatially constrained fragments of MOF crystals. Real MOF samples frequently contain defects and display crystal-size-dependent phenomena^{36,37} on which insight is only attainable by taking time-resolved experimental measurements of the system during the dynamic events. By monitoring at time intervals that are sufficiently short to capture the dynamic phenomena in question, key information within transiently accessed, non-equilibrium states can be obtained. In turn, this information facilitates piecing together the nature of the potential energy surface describing the flexible framework during its contortions. The ultimate goal is to allow the rational design of flexible “4-dimensional frameworks” with deliberate and predictable time-dependent properties, a goal that was expertly set out by Kaskel et al. in 2020³⁸ and beautifully framed in conceptual terms. The biggest hurdle to achieving this goal is still obtaining detailed experimental information with which to experimentally apply the conceptual framework.

In this review, we provide the reader with a contemporary picture of the state of experimental MOF research in the time domain. After dividing the field into four subsections, we use a technique→phenomenon→framework approach. By putting the techniques at the forefront of the discussion, we hope to demonstrate their utility in the study of time-resolved MOF dynamics and to highlight several newer or less well-known techniques (Table 1, Figure 1).

The four subsections of the field we describe are based on the type of motional behaviour investigated. In one sense, the most dynamic of behaviours is of course the synthetic process itself. Beginning with “MOF Formation”, therefore, we describe time-resolved techniques that monitor the MOF synthesis process, followed by “Guest Motion” where we discuss the time-resolved study of guest translational motion throughout MOF pores. The third section covers the perhaps more esoteric but no less important phenomena of “Electron Motion”, describing charge transfer and conductivity in MOFs. Having looked at how MOFs form and what goes on inside them, finally, we describe studies on “Framework Motion” itself.

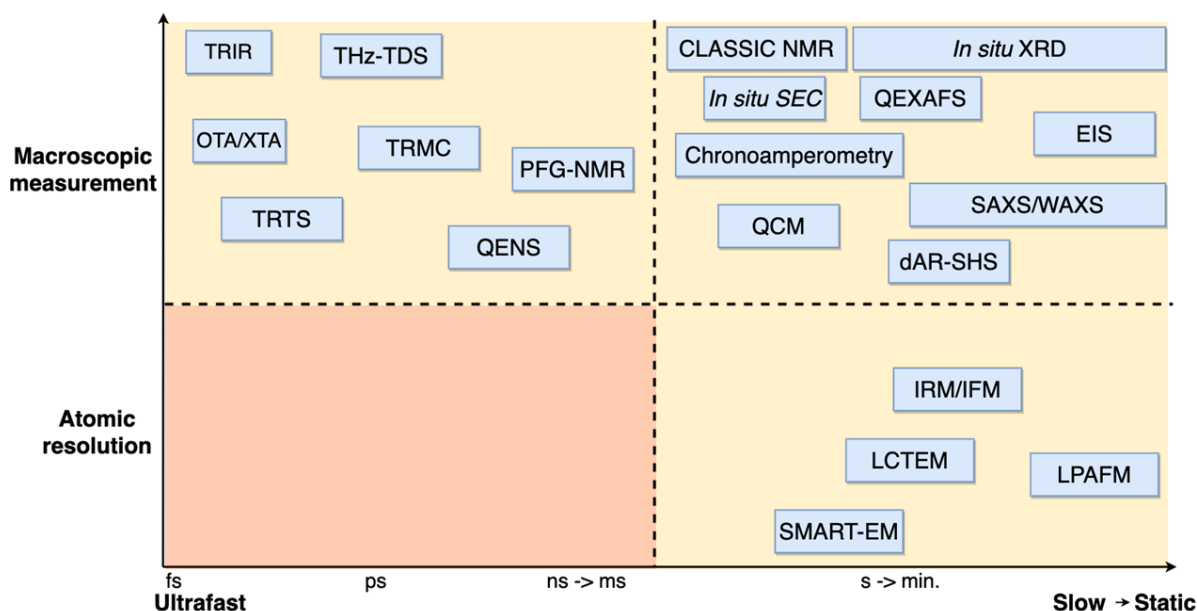


Figure 1. Methods described in this review to investigate dynamic phenomena in MOFs. The techniques are arranged into quadrants according to the spatial and temporal resolution achievable in the measurement. To date, no technique has been developed that can study MOFs with both ultrafast and atomic resolution. If one were to emerge, it would be truly revolutionary.

Technique name	Acronym	Working principle	Typical time resolution	Information provided
Upper-left quadrant in Figure 1				
Time-resolved infrared	TRIR	An optical-pump infrared-probe technique. The vibrational spectrum is recorded as a function of time elapsed since optical excitation.	fs to μm	TRIR records time-dependent changes in the vibrational spectra of excited state species. This can provide insight into photoinduced transition states, charge transfer dynamics and the photocatalytic mechanisms of MOFs.
Terahertz time-domain spectroscopy	THz-TDS	THz-TDS uses a pulsed laser split between sample and delay line and recombined at a detector to yield the THz signal in the time domain, which Fast Fourier Transform (FFT) converts to the THz spectrum in the frequency domain.	ps	Provides information on collective lattice vibrations (phonon modes) which are key to understanding MOF mechanochemical properties in different phases and in the presence/absence of guests. THz-TDS is advantageous since conventional Fourier transform vibrational spectroscopies have poor resolution in the THz region and lack the amplitude and phase information of THz-TDS.
Optical transient absorption	OTA	Optical-pump optical-probe technique. The sample is excited using an optical pump and then the photogenerated states are measured using an optical probe at different times after excitation.	fs to μs	Yields time-dependent optical absorption spectra. Provides a wealth of information regarding the electronic properties of transiently accessed photoexcited states including MOF relaxation dynamics and charge transfer processes.
X-Ray transient absorption	XTA	Optical-pump X-ray-probe technique. Unlike OTA, XTA measures the X-ray absorption spectrum of photogenerated excited state species.	fs to μs	XTA provides time-resolved information regarding the electronic structure and chemical environment around metal nodes in MOFs in photoexcited states. The technique requires short X-ray pulses normally obtained using synchrotron radiation
Time-resolved microwave conductivity	TRMC	The sample is excited using an optical pump pulse and time-resolved photoconductivity is measured by recording changes in recorded microwave power with respect to the time delay after excitation.	ps to ns	TRMC permits transient photoconductivity to be measured on extremely short time and length scales. This provides so called "intrinsic" conductivity of the sample. As a "non-contact" method, grain boundary and random orientation effects common in contact measurements of conductivity are avoided.
Time-resolved terahertz spectroscopy	TRTS	Similar to TRMC, except changes in THz transmission through the sample are measured instead of microwave power.	fs	TRTS also permits transient intrinsic conductivity measurement, except the time resolution is superior to TRMC.
Pulsed-field gradient nuclear magnetic resonance	PFG-NMR	A constant magnetic field B_0 is superimposed, over two short time intervals δ of separation t , by an additional, inhomogeneous field $B_{\text{add}}=g_x$ (the field gradients). This results in the NMR signal being transferred into the distribution function of the nuclear spins under study in the x direction. The signal attenuation of the signal intensity with and without the field yields an expression that relates transport diffusion D_t to the mean square displacements $\langle x^2 \rangle$.	ns to ms	Since the technique interrogates the mobile components of the sample, guest diffusion over ns-ms timescales within MOFs can be calculated from these measurements. There is no directly obtained spatial resolution in the measurement.
Quasi-elastic neutron scattering	QENS	Neutrons are fired at the sample. The number of scattered neutrons is counted as a function of scattering vector \mathbf{q} and energy transferred $\hbar\omega$. The broadening of the "elastic" peak is caused by the dynamics of the system, so by fitting the shape of this peak, the diffusion coefficient, D , can be obtained.	ps	Like PFG-NMR, QENS also provides guest diffusivity via measuring average time-dependent particle displacements. However, QENS has superior time- and (indirect) spatial-resolution (ps and nm), although typically larger sample quantities are required and the measurement is slower than PFG-NMR to perform due to the relatively low flux of most neutron sources.
Upper-right quadrant in Figure 1				
Combined liquid- and solid-state in-situ crystallisation NMR	CLASSIC NMR	A type of in-situ NMR method whereby the solid and liquid phases are alternately interrogated over time, with the liquid phase being 'invisible' to the solid phase measurement and vice versa. Time resolution depends on the nuclei being studied.	min to h	This is a good method for looking at early nucleation/crystal growth because one can analyse the depletion of solution species simultaneously with the growth of solid particles.

In-situ X-ray diffraction	In-situ XRD	In-situ XRD encompasses both in-situ powder XRD (PXRD) and in-situ single-crystal XRD (SCXRD). These techniques yield spatially averaged information on macroscopic samples that in turns can provide averaged atomistic structural information.	s to h	Structural information on MOFs during crystallisation processes, framework structural changes and changes to MOFs occurring during guest/electron diffusion. Angular-dispersive XRD (ADXRD) can achieve time resolution on the order of seconds, which makes it very useful in the study of the kinetics of MOF formation.
In-situ Spectro-electrochemistry	In-situ SEC	<i>In-situ</i> spectroelectrochemistry (SEC) describes the combination of both spectroscopic and electrochemical experiments, typically by incorporating appropriately transparent windows in a thin electrochemical cell, which is then mounted in the spectrometer. MOF thin films on transparent electrodes are the most common approach to sample mounting.	s	The electrochemical cell initiates a redox process which is then followed by spectroscopic techniques such as Raman/IR, electron paramagnetic resonance (EPR) and UV/Vis spectroscopy. This enables phenomena such as charge transport and ion/electron mobility in MOFs to be investigated as long as they can be mounted on the working electrode.
Quick-scanning extended X-ray absorption fine structure	QEXAFS	EXAFS exploits the scattering and interference of electrons, excited into continuum states from the atomic core, off the neighbouring atoms and measures the interference as a function of energy. QEXAFS is time-resolved EXAFS. It enables the in-situ study of time-dependent changes in local chemical environment about metal centres.	min	The ability to probe the chemical environment around metal centres, to yield number, type and distances of neighbouring atoms to those studied, with a time resolution of minutes is particularly useful in the study of MOF formation. QEXAFS can be used to study the very earliest stages of MOF nucleation, where insights via X-ray approaches are inaccessible due to the small sizes and non-crystalline nature of the species present.
Chrono-amperometry	CA	In chronoamperometry, a voltage is applied to the sample and the resulting current response is measured as a function of time.	ms to min	Chronoamperometry can be used to investigate guest/electron diffusion in MOFs from the current response vs time plots.
Electrochemical impedance spectroscopy	EIS	A MOF sample (often a pressed disc) is connected to electrodes and an AC potential is applied. The resulting current signal is measured, and impedance (Z) is calculated from an approximation of Ohm's Law. A Nyquist plot of the imaginary (Z'') vs real (Z') impedance components is then fitted to an 'equivalent circuit' that permits calculation of the proton conductivity.	min	EIS is useful for investigating ion and electron conductivity in MOFs. It, like many other "contact methods" suffer from grain boundary and random orientation effects due to the sample form and preparation.
Quartz-crystal microbalance	QCM	The MOF sample is placed on a very sensitive quartz crystal balance. The Sauerbrey equation relates changes in overtone frequency of the quartz crystal to mass loading. Gases are introduced to or removed from the MOF sample and the resulting mass changes are measured.	s	The time-dependent guest-induced mass changes of the sample are analysed in the frame of Fickian diffusion whereby the normalised mass loading at time t is directly related to guest diffusivity. The high sensitivity of QCM is useful for investigating time-dependent guest uptake/release kinetics and guest diffusion as well as surface barriers in MOF crystals and thin-films.
Small-angle X-ray scattering	SAXS	SAXS measures X-ray scattering at low angles thus providing information on particle size and shape in solutions and suspensions. SAXS does not rely on long-range order (unlike diffraction methods), therefore it is sensitive to amorphous species.	s to min	Size and shape information on MOF particles of sizes 1-100 nm. This is smaller than the detection limit for XRD, therefore it is a complementary technique to XRD in the study of MOF formation.
Dynamic angle-resolved second harmonic scattering	dAR-SHS	dAR-SHS is a second-order nonlinear optical technique that interrogates solutions and suspensions. Single-shot measurements of the second harmonic signal at multiple angles in a Fourier-imaging scheme allows for simultaneous measurement of size, shape, and concentration of scattering species.	s	dAR-SHS is an emerging technique and has not been used very extensively in the field. Where it has been used it has helped elucidate MOF formation mechanisms. dAR-SHS provides symmetry information for individual molecules all the way up to small crystallites, meaning early-stage MOF nucleation and growth can be monitored.
Lower-right quadrant in Figure 1				
Infrared microimaging	IRM	In IRM, the primary measurement is the changes in the IR spectrum of a MOF crystal using a microscope to provide spatial resolution down to a few microns. Characteristic bands of the guest molecule under study can be monitored over time and correlated to local concentration of the guest.	s to min	Guest flux gradients in one or two spatial dimensions can be measured during guest uptake and release to provide a "real time" diffusion map in individual MOF crystallites. Additionally, IRM permits simultaneous measurement of multiple species, making it particularly powerful for multicomponent diffusion analysis.

Interference microscopy	IFM	IFM is a method of monitoring the evolution of transient guest concentration profiles during uptake and/or release. IFM exploits the fact that the refractive index of a sample, n_1 , depends on the guest concentration. Changes in local concentration, $c(x, y, z; t)$ are proportional to changes in refractive index of the sample $n_1(x, y, z; t)$ meaning the recorded interference patterns lead directly to plots of concentration integrals over the crystal.	s to min	IFM, like IRM, measures guest concentration gradients over a MOF sample in one or two dimensions. The spatial resolution of IFM, dependent on the optical probe wavelength, is superior to IRM, but simultaneous measurement of different species is not possible.
Liquid cell transmission electron microscopy	LCTEM	LCTEM measures surface structure of MOF crystals by capturing 2D images of the surface using an electron beam with a scan rate that yields a time resolution of a few seconds. Unlike conventional TEM instruments, LCTEM can operate in solution.	s	LCTEM has primarily been used to study MOF formation. Since it can operate in solution and has a spatial resolution on the order of nanometres, nucleation and particle growth can be investigated.
Liquid phase atomic force microscopy	LPAFM	LPAFM provides the nanoscale structure of a sample surface. An AFM tip raster scans the sample surface in the (xy) plane and generates a 3D topological surface map by measuring the differences in intermolecular forces in the z-direction between the scanning tip and the surface atoms. LPAFM can operate in solutions as well as on solid samples, visualising solution phase surface processes in real time with nanometre spatial resolution.	min	Used to look at growing MOF surfaces and thin films, as well as looking at changes to MOF surfaces as a result of guest adsorption from solution. The technique can aid characterisation of MOF surface termination and defects.
Single-molecule atomic-resolution real-time electron microscopy	SMART-EM	SMART-EM is a TEM-based technique whereby real-time atomically-resolved images of a sample surface can be captured. The technique involves a process of "fish hooking" of the particle of interest with a suitable "fishing rod" (typically a small organic molecule attached to a carbon nanotube).	s to min	Like LCTEM, SMART EM enables real-time imaging of MOF formation, particularly in the early stages of formation such as solution phase and pre-nucleation dynamics.

Table 1. All the techniques presented in Figure 1, along with their corresponding acronyms, basic working principle, typical time resolution and utility in the context of MOF dynamics.

The studies described below represent important progress in the ongoing investigation of MOFs in the time domain, but such studies form just a tiny fraction of the vast existing MOF literature. Given the wealth of critically important information that is accessible by considering dynamic behaviours of MOFs, if they are to be fully exploited for their scientific and commercial potential this situation has to change.

MOF Formation

The making of a MOF begins on the nanoscale, with metal-ligand complex formation, and leads all the way up to macroscale particle growth and bulk material production. MOF formation relies upon the ultrafast bond-breaking and making processes of self-assembly and supramolecular chemistry, which ultimately follow through to crystal growth on timescales of seconds to days. No single technique can interrogate the complex manifold of species in a MOF synthesis from femtoseconds to days, but each process in the intricate ballet of framework construction will impact on the product that forms and on the properties it possesses. Synthetic method, particle size, morphology, defect content, surface chemistry and phase behaviour all play their part in the final material, and all stem

from the formation process.³⁹⁻⁵⁰ Understanding MOF formation is key to unlocking true function-led design of MOFs in the future.

The breadth of this challenge is summarised in Figure 2. The use of *in-situ*, time-resolved techniques to study MOF formation has been reviewed extensively by others quite recently, a notable example being that of Van Vleet *et al.* in 2018.⁵¹ However, this is a fast-moving research arena and therefore in this section we discuss the key cutting-edge experimental techniques in the field. The most recent studies are discussed in the context of more established methods.

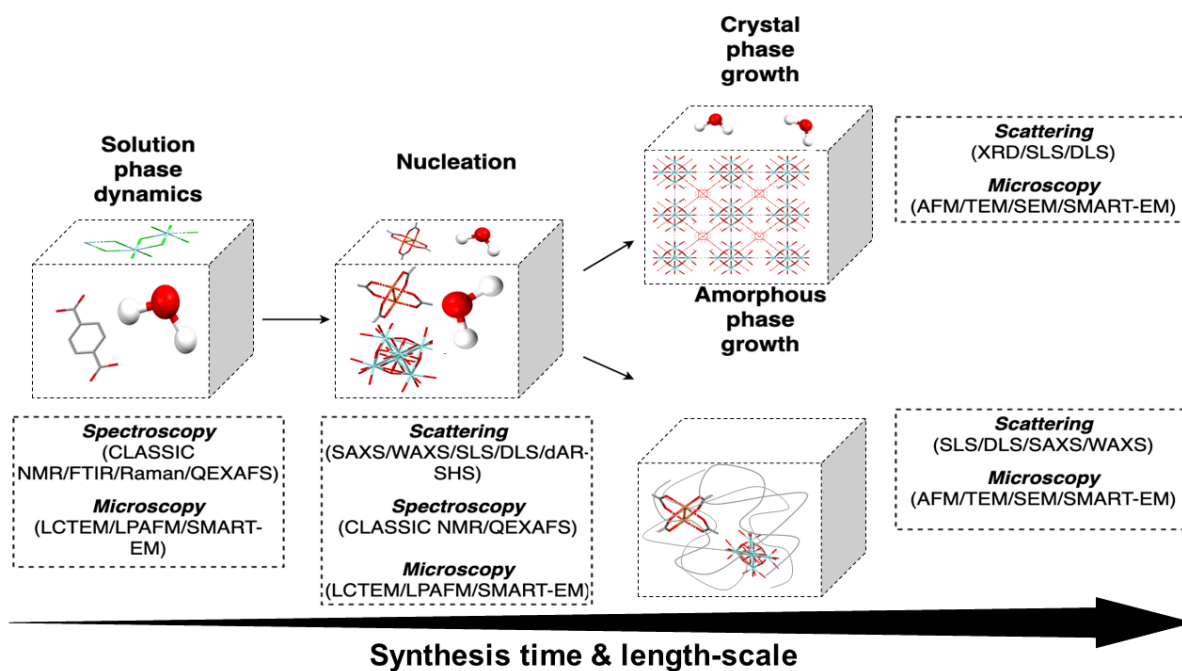


Figure 2. Schematic depicting the MOF synthesis reaction and the dynamic techniques used to probe each stage. Spectroscopic techniques and adapted liquid-phase microscopy are ideal for studying early stage, solution phase phenomena such as the formation of prenucleation clusters. When particle size increases beyond that required to scatter light efficiently, techniques like small-angle X-ray scattering (SAXS), wide-angle X-ray scattering (WAXS), static light scattering (SLS), dynamic light scattering (DLS) and dynamic angle-resolved second harmonic scattering (dAR-SHS) become useful probes for monitoring particle size/shape and symmetry during nucleation. As the reaction continues, crystalline phases capable of diffracting light form and are thus analysed by X-ray diffraction techniques like angular-dispersive X-ray diffraction (ADXRD) and energy-dispersive X-ray diffraction (EDXRD). Non-diffracting, amorphous phases can also form, and these can be instead analysed by light scattering and microscopic techniques.

X-ray scattering methods (XRD, SAXS) (timescale: seconds to hours)

Diffraction methods provide information on late-stage MOF formation when crystallites of sufficient size and structural order to diffract are formed. The most common model applied to crystallisation data is the Gaultieri model, which describes the process using parameters of nucleation rate k_n and crystal growth rate, k_g .⁵² Traditionally, the faster acquisition time of energy-dispersive X-ray diffraction (EDXRD) resulted in it being the method of choice for early studies,^{53,54} but developments in detector technology have triggered the emergence of *in-situ* angular-dispersive X-ray diffraction (ADXRD) as well.⁵⁵⁻⁵⁷

A prime example of the utility and impact of *in-situ* EDXRD was a report in 2014 by Ragan *et al.* on UiO-66(Zr) formation.⁵⁸ Ragan *et al.* used *in-situ* EDXRD to study the crystallisation kinetics of UiO-

^{66}Zr) with a 30 s time resolution. Three key experimental observations were made: addition of water increases the crystallisation rate constant and yield; addition of HCl does the same but to a lesser extent, and use of $\text{ZrOClO}_2 \cdot 8\text{H}_2\text{O}$ instead of ZrCl_4 as precursor slowed crystallisation but afforded a higher product yield. The same group subsequently reported that changing linker length and functionalisation had a temperature-dependent impact on the crystallisation rate of the analogous isorecticular frameworks as a result of differing linker solubilities in the reaction.⁵⁹

Not all frameworks form as single-phase, phase-pure materials.⁶⁰⁻⁶² Cutting-edge ADXRD experiments at the Diamond synchrotron with data collected every 4 seconds enabled a particularly notable study of a complex system, reported by Yeung *et al.*⁶³ They were able to describe the energetics of lithium tartrate MOF crystallisation, quantifying the rate constants and activation barriers for formation, dissolution and conversion of each component in the energy landscape. Crystallisation was governed by an equilibrium between intermediate species, with the inference being that changes in ligand conformation might play a rate-limiting role in the formation of MOFs with flexible linkers. In more rigid examples such as ZIF-8, studied in 2019 by the same group,⁶⁴ the impact of metal ion concentration on nucleation and crystal growth rates was examined; the authors derived a model whereby prior to ZIF-8 network assembly, a pre-equilibrium exists between metastable intermediate clusters with varying Zn:mIM (mIM = 2-methylimidazolate) ratios and degrees of protonation. This pre-equilibrium is concentration dependent and determines the rate of crystallisation, meaning that concentration can be used as a handle to directly control particle size.

X-ray diffraction methods are limited by the need for diffracting particles. Small-angle X-ray scattering (SAXS), however, can shed light on the formation and behaviour of pre-diffraction and amorphous species.^{65,66} Carraro *et al.* used synchrotron time-resolved SAXS with a 100 ms time resolution to monitor the nucleation, growth and crystallisation of ZIF-8 encapsulated with bovine serum albumin (BSA@ZIF-8) in a continuous flow synthesis.⁶⁷ SAXS data reported on the growth of non-diffracting species over the first 3 minutes of the synthesis (on length scales up to 35 nm), after which crystalline BSA@ZIF-8 formation began to dominate, observed by the growth of the (110) Bragg diffraction peak and loss of the amorphous scattering. SAXS has also been used to monitor the homogeneous nucleation and early crystal growth events taking place during ZIF-8 formation,⁶⁸ to investigate the kinetics of multiphase growth of $\text{NH}_2\text{-MIL-53}$,⁶⁹ and to study the entire ZIF-71 nanocrystal formation mechanism.⁷⁰

Many MOFs have been synthesised by mechanically grinding/milling/shearing dry reagents together, in the absence of any solvents: this is known as mechanosynthesis, a particularly green method for synthesising MOFs which is on the rise.⁷¹ In-situ measurement of the mechanochemical MOF synthetic process is extremely challenging given the nature of the method, but X-ray and spectroscopic methods have been employed in a few cases that have recently been reported and reviewed.^{72,73,74}

The examples in this section demonstrate the utility of X-ray methods for the mechanistic analysis of MOF formation but are ultimately limited in their scope by requiring particles large enough to scatter (typically 1 – 100 nm for SAXS)⁷⁵ or diffract (typically >5-10 nm for powder diffraction patterns, >10 μm for single-crystal structure solutions).^{76,77} Additionally, despite the atomistic information provided by X-ray crystallography, X-ray techniques measure spatially averaged data, providing bulk-average information with local structural irregularities invisible to these methods.

Microscopy (timescale: seconds to minutes)

Microscopy techniques can be used to interrogate surface phenomena and local structural changes instead of spatially averaged structural features.^{78,79}

Zheng *et al.*⁶² monitored the growth of MOF-5 by taking scanning electron microscopy (SEM) images with a time resolution on the order of hours. They conclude that MOF-5 nucleation does not take place in the solution, but inside $Zn_5(OH)_8(NO_3)_2 \cdot 2H_2O$ -1,4-BDC (BDC = 1,4-benzenedicarboxylate) particles. They identify the basic building units for the construction of MOF-5 cubes as small MOF-5 crystallites which self-assemble into porous microcubes. These then undergo surface-recrystallisation and reversed crystal growth to yield cubic single crystals of MOF-5. This study highlights how *in-situ* SEM can relate MOF morphology to physicochemical properties.

A recently developed technique, single-molecule atomic-resolution real-time electron microscopic (SMART-EM) video imaging, was used to investigate early-stage MOF nucleation.⁸⁰ Taking images at a rate of two frames per second, the authors identified two prenucleation clusters (PNCs) involved in the formation of MOF-2 and MOF-5 at 95 °C and 120 °C respectively. The shape of these PNCs differed in each case, suggesting that MOF-2/5 bifurcation occurs early, in the PNC stage. Prior to this study, MOF-2/-5 PNCs were identified only by mass spectrometry. Earlier *in-situ* studies using light scattering could only reveal small crystallites, lacking the spatial resolution to image the PNCs themselves.⁸¹

Liquid-cell transmission electron microscopy (LCTEM) allows for the direct probing of MOF solution phase dynamics as well as solid-phase growth. With a time resolution on the order of seconds, Patterson *et al.* used *in-situ* LCTEM to study the nucleation and crystal growth of ZIF-8. LCTEM images showed that by tuning the metal:ligand ratio, crystal size can be controlled. The authors also show that the nucleation process is limited by local depletion of monomers, whereas growth is a surface-limited process.

In-situ atomic force microscopy (AFM) was employed by Moh *et al.* to further probe the crystal growth process of ZIF-8.⁸² With a time resolution of minutes and a spatial resolution on the order of nanometres, growth was shown to occur by a “growth and spread” mechanism, eventually forming stable surface steps of the enclosed framework structure. A recent study by Mandemaker *et al.* studied the kinetics of both nucleation and crystal growth of HKUST-1 thin films using *in-situ* liquid-phase AFM (LPAFM) with a time resolution of 15 min.⁸³ At 25 °C, initial nucleation of rapidly growing HKUST-1 islands was surrounded by a continuously nucleating but slowly growing HKUST-1 carpet.

Microscopy allows for time-resolved (seconds to minutes) and spatially-resolved (down to atomic resolution) data on crystal growth as well as amorphous phase growth and PNC dynamics. LCTEM and LPAFM are particularly powerful as they are capable of operating in solution; enabling both early-stage dynamics and solid-phase growth information to be obtained directly.

Light scattering (timescale: seconds to minutes)

Static light scattering (SLS), which records the intensity of light scattered by the sample at a range of angles, and dynamic light scattering (DLS), which records the fluctuations in scattering intensity over time, are sensitive to scatterers of sizes ≥ 1 nm, require homogenous solutions and are a valuable tool for the study of early-stage solution processes.⁸⁴ Van Vleet *et al.* have done an excellent job of reviewing the utility of SLS and DLS within the frame of MOF early-stage nucleation.⁵¹ Consequently, here we focus on a newer light-scattering technique: angle-resolved second harmonic scattering (AR-SHS). This is a second-order nonlinear optical technique that is capable of simultaneously measuring the size, shape, and concentration of scattering species.⁸⁵ Additionally, polarisation-resolved measurements enable the symmetry of the scattering species to be probed. In order to achieve adequate time resolution, Van Cleuvenbergen *et al.* developed a method of taking single-shot measurements of the second harmonic signal at multiple angles by imaging a large portion of the AR-SHS pattern on an electron multiplying charge coupled device camera in a Fourier-imaging scheme (dynamic angle-resolved second harmonic scattering, dAR-SHS).⁸⁶ dAR-SHS was used to

monitor the formation of ZIF-8 (T_d symmetry) with a time resolution of 3 s, simultaneously measuring size, shape, and concentrations of intermediate species. dAR-SHS provides symmetry information for individual molecules up to small crystallites, meaning the earliest stages of nucleation can be probed. The beauty of this technique is the fact that detection of the scattered light requires no moving parts, making measurements inherently quick and suitable for *in-situ* monitoring of MOF formation.

QEXAFS (timescale: seconds to minutes)

While the techniques discussed thus far allow for the study of MOF nucleation and crystal growth on multiple length- and time-scales, they do not provide much local chemical information in the early complexation stages. Quick-scanning extended X-Ray absorption fine structure (QEXAFS) does exactly this by directly probing changes in the coordination environment of metal centres as a function of time.⁸⁷ Goesten *et al.* used QEXAFS to study ZIF-7 crystallisation with a time resolution of ~ 100 s.⁸⁸ When the benzimidazolate linker is added, there is a shift in equilibrium from 6-coordinated O_h zinc to 4-coordinated T_d zinc. Contrary to previous hypotheses, this increase in T_d zinc does not represent ZIF-7 formation, which is instead initiated by addition of the diethylamine modulator.

CLASSIC NMR (timescale: minutes)

Another relatively new technique, known as combined liquid- and solid-state *in-situ* crystallisation NMR (CLASSIC NMR), first introduced by Hughes *et al.*, also provides time-resolved molecule-level information.⁸⁹ CLASSIC NMR monitors both the solid-phase and liquid-phase simultaneously and can be carried out on a standard solid-state NMR spectrometer. In a study by Jones *et al.*, CLASSIC NMR was used to study the nucleation and growth of MFM-500(Ni), particularly in the early stages of MOF nucleation.⁹⁰ Fitting the time-resolved liquid-phase ^1H data to the two-stage model of Gualtieri allowed for the activation energies of nucleation (61.4 ± 9.7 kJ mol $^{-1}$) and growth (72.9 ± 8.6 kJ mol $^{-1}$) to be determined. While the CLASSIC method was used, the solid-state spectra were not utilised because the liquid-phase data was far more interesting. This presents an opportunity to explore the technique further in the future.

In-situ vibrational spectroscopy (timescale: milliseconds to minutes)

Like QEXAFS and CLASSIC NMR, another approach that provides chemical insight into early-stage dynamics of the MOF formation processes is *in-situ* vibrational spectroscopy. Zhao *et al.* studied the kinetics of HKUST-1 thin film growth using *in-situ* attenuated total reflection Fourier-transform infrared spectroscopy (ATR-FTIR).⁹¹ The data revealed the formation of (Zn, Cu) hydroxy double salts (HDSs) from ZnO thin films and conversion of HDSs to HKUST-1. Additionally, their flow-cell apparatus can be easily applied to other solid/liquid reaction systems. Embrechts *et al.* investigated the formation mechanism of MIL-53(Al) via simultaneous *in-situ* Fourier-transform infrared spectroscopy (FTIR) and *in-situ* Raman spectroscopy.⁹² While inelastic neutron scattering (INS) can give the vibrational spectrum of a material without the selection rules of Raman or IR spectroscopies,¹³ the combined use of FTIR and Raman measurements by Embrechts *et al.* allows all vibrational bands to be observed without the need for a neutron source. The authors identified a prenucleation building unit (PNBU) consisting of one linker and one Al atom and monitored the evolution of nuclei in solution through to final precipitation of the crystalline MOF phase. The same group investigated the mechanism of bifurcation of MIL-68(Al) and MIL-53(Al).⁹³ In their experiments MIL-68(Al) was favoured over MIL-53(Al) due to the combination of a deficiency of terephthalic acid in solution and a slow MOF growth rate. Formic acid slowed down prenucleation and crystal growth by forming hydrogen bonds with the carboxyl group of the terephthalic acid linker, not by competitive metal coordination.

Concluding remarks

MOF formation is a dynamic and complex process occurring on multiple different length-scales and timescales. A thorough understanding of the whole process is only achieved with a combinational approach whereby techniques operating in different space and time domains are used in tandem. X-ray techniques and are key for tracking crystal growth, while microscopy is useful for understanding local changes and surface phenomena. Early-stage, molecular-level phenomena such as solution-phase dynamics and prenucleation cluster formation is gained through NMR/QEXAFS/spectroscopic methods.

Guest motion

The motion of guests throughout MOFs is of crucial importance to their potential applications in gas storage, separation as well as in drug delivery and conductive membranes.⁹⁴⁻⁹⁷ Herein we review techniques that measure the translational diffusion of guests (Figure 3), including the smallest possible guest: the phenomenon of proton conduction.

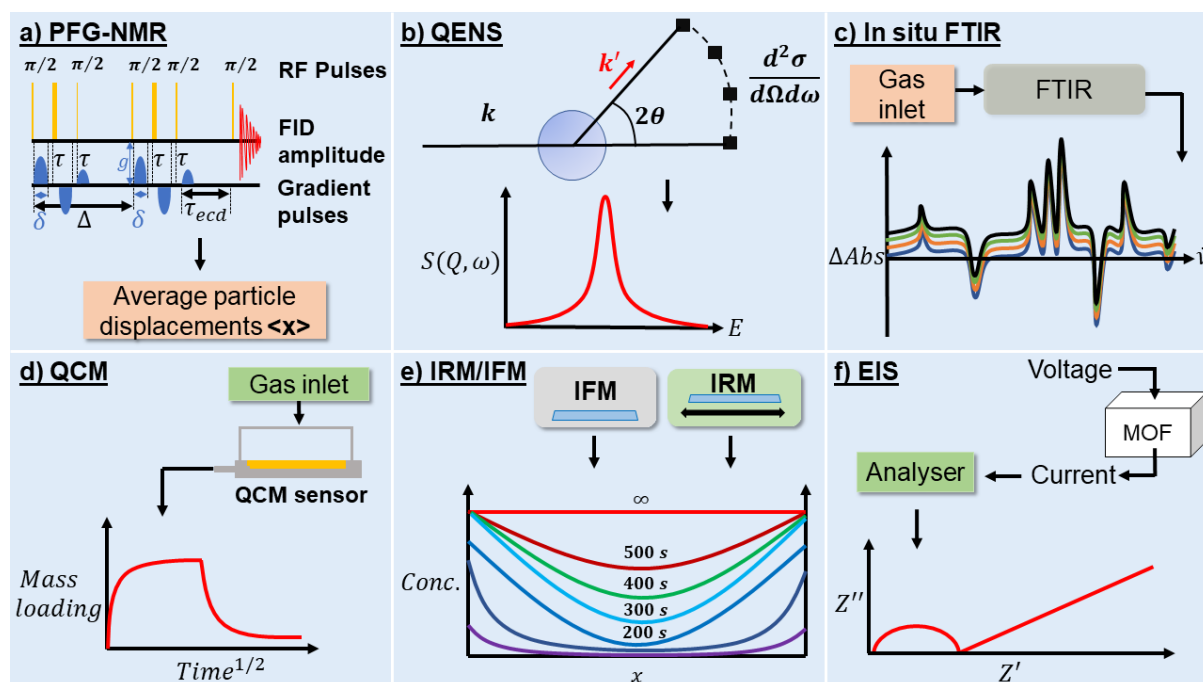


Figure 3. Experimental techniques for the study of translational guest diffusion in MOFs. a) pulsed-field gradient nuclear magnetic resonance (PFG-NMR) uses additional inhomogeneous gradient pulses to extract the mean square displacement of particles over time between pulses, t ; b) quasi-elastic neutron scattering (QENS) also gives average particle displacements over a specified time, permitting the calculation of diffusion coefficients; c) FTIR monitors intensity and frequency changes in the vibrational spectra of host and guests over time, and fitting the time-dependent changes in IR intensity to diffusion models (e.g. Fickian diffusion) permits calculation of relevant diffusion coefficients; d) quartz crystal microbalance (QCM) probes guest adsorption and desorption kinetics by measuring the change in mass during a guest uptake or release process; e) interference microscopy/infrared microimaging (IFM/IRM) measure transient guest concentration profiles across individual MOF crystals; f) electrochemical impedance spectroscopy (EIS) measures electrical

impedance to generate Nyquist plots which are then used to derive sample ion and/or electron conductivity.

PFG-NMR (timescale: nanoseconds to milliseconds)

Pulsed-field gradient NMR (PFG-NMR) offers molecular translational diffusion information with millisecond time resolution and micrometre length scales.⁹⁸⁻¹⁰⁰ Multinuclear magic-angle spinning (MAS PFG-NMR) was employed by Chmelik *et al.* to study the selectivity of ZIF-8 towards an ethene:ethane gas mixture.¹⁰¹ Historically, much gas selectivity has been inferred from single-component sorption isotherms and studies investigating mixtures are still in the minority.¹⁰² PFG-NMR can do this directly and gives more information. The study reports $D_{\text{ethene}}:D_{\text{ethane}}$ selectivity of 5.5 showing that ZIF-8 is an effective separation medium for a mixed-gas stream containing these gases. Activation barriers derived from this data showed that selectivity is guest-size dependent, almost independent of host-guest interactions. Considering guest-guest interactions, Freude *et al.* used MAS PFG-NMR to study propene diffusion through ZIF-8.¹⁰³ Propene diffusion was independent of the presence of propane (up to 1:4 loading), contradicting observations in zeolites where the diffusivity of smaller species is impeded by the presence of larger species.¹⁰⁴ Framework flexibility itself may also have enhanced guest diffusion rates. Guests are not always 'innocent': Forman has shown that in streams of methane and CO₂, an increase in diffusion *time* led to a decrease of diffusion *rate* in ZIF-11.¹⁰⁵ This is because the guest molecules bound to the pores walls "deflect" other molecules and prevent entry into the pores of the framework.

In 2018, Forse *et al.* used PFG-NMR to study the diffusion of CO₂ in channel-containing Zn(dobpdc) (dobpdc = 4,4'-dioxido-3,3'-biphenyldicarboxylate) in 2 crystallographic directions.¹⁰⁶ Surprisingly, CO₂ diffusion perpendicular to the channels was 30x less than diffusion through the channels, but not zero. Given the kinetic diameter of CO₂ (3.3 Å) compared with the maximum pore size in the *ab* plane (0.6 Å), the authors conclude that diffusion perpendicular to the channels occurs through defects, rather than by the framework distorting to allow CO₂ passage. Work by Popp *et al.* showed that it is possible to tune the self-diffusivity of solvents linearly between the diffusivity in MOF-5 and IRMOF-3 by varying the solvent mole fractions.¹⁰⁷ Intermolecular attractive forces between the MOF and guest played a comparatively minor role, with steric effects of pore-aperture size changes being the predominant factor.

More recently Walenszus *et al.* employed PFG-NMR to examine the impact on guest diffusion in the highly flexible MOF DUT-49(Cu) caused by drastic phase changes brought on by increasing the loading of the guest.¹⁰⁸ DUT-49 has two main structures, open pore (op) and closed pore (cp), with vastly different guest diffusion properties. By using in-situ PFG-NMR supported by molecular dynamics simulations, the change from op to cp was observed as a change in n-butane diffusivity as the applied pressure of n-butane changed from 35.7-37.4 kPa; upon saturation of all pores with n-butane the observed diffusivity dropped 4-fold. This change gives rise to the fascinating phenomenon of negative gas adsorption (NGA). The work represents an innovative method for indirectly monitoring changes in MOF structure without directly following the framework structure change itself (e.g. by crystallographic methods).

The emergence of PFG-NMR for measuring guest diffusion has revealed an apparent dominance of steric effects over both host-guest or guest-guest electronic effects on the rates of guest transport in MOFs. Most studies have focussed on characterising the diffusion of industrially relevant gas streams and a challenge for the future is to investigate more chemically complex guest molecules where host-guest and guest-guest interactions define or even control molecular diffusion. Examples characterised with other techniques do exist, such as those described in the QENS section below.

In-situ FTIR (timescale: milliseconds to minutes)

Monitoring the changes in the vibrational spectra of guests as a function of time during diffusion provides complementary information to that obtained by PFG-NMR measurements. The growth and decay of features during guest uptake/diffusion permits diffusivity calculations while analysis of frequency shifts provides mechanistic insight into the diffusion mechanism and guest-host interactions.¹⁰⁹⁻¹¹³

Sharp *et al.* used this technique to monitor Fickian diffusion of butane in UiO-66.¹¹⁴ The data showed the intensity of $\nu(\text{MOF-OH})$ bands decreasing as $\nu(\text{MOF-OH-alkane})$ hydrogen bonding bands grow. From this *in-situ* data, the preferential binding site of n-butane in UiO-66 was elucidated, diffusion coefficient was calculated, and the activation energy of diffusion was calculated along with a suggestion of the diffusion-limiting step. Benzene, toluene, and *o-/m-/p*-xylene diffusion in the same host were investigated by Grissom *et al.* who were interested in the entropic and steric effects on diffusion.¹¹⁵ Using *in-situ* FTIR, the authors found that diffusion decreased in the order benzene \sim toluene $>$ *p*-xylene $>$ *m*-xylene $>$ *o*-xylene, agreeing with several studies discussed earlier that steric effects play a major role in diffusivity.

QENS (timescale: picoseconds to nanoseconds)

QENS is a neutron scattering technique where the transfer of energy from the incident neutron to the analyte is small. When fitted to the appropriate Lorentzian function, QENS data yields, like PFG-NMR, average particle displacements however with improved spatial and temporal resolution.^{116,117}

Kolokolov *et al.* investigated the mechanism of benzene diffusion through MIL-47/-53 using QENS/MD.¹¹⁸ In the flexible MIL-53(Cr) a guest-induced transition from an *op* \rightarrow *np* state is observed before benzene diffusion via a 1-D hopping mechanism. Conversely, in the rigid MIL-47(V), diffusion occurs via a tumbling, corkscrew-like motion that is disfavoured in the flexible framework due to activation energy barriers. This is in contrast to work by Rosenbach *et al.* in which the QENS data for methane diffusion in the same frameworks showed greater diffusivity in MIL-47(V), proposed to be due to stronger guest-host interactions in the latter.¹¹⁹

The use of QENS in the analysis of MOF-guest interactions is not limited to unimolecular systems. Yang *et al.* investigated the co-diffusion mechanism for a CO_2/CH_4 mixture through UiO-66.¹²⁰ The diffusion was found to be different to that observed in zeolites in that inclusion of CO_2 in the MOF pores actually increased the rate of diffusion.¹²¹ The combined QENS/molecular dynamics (MD) data showed that inclusion of CO_2 in the MOF pores did not retard CH_4 diffusion, but instead allowed for faster CH_4 diffusion by impeding the attractive CH_4 -host interactions. This fascinating outcome is in direct contrast to the behaviours observed for CH_4 and CO_2 in ZIF-11 as measured by PFG-NMR when the diffusion rate changes were ascribed to purely steric effects.¹²² The metal nodes in both UiO-66 and ZIF-11 are coordinatively saturated, so this difference in behaviour is striking.

In 2019 QENS/MD revealed a new type of non-Fickian diffusion in MOFs: diffusion of neo-pentane in MIL-47(V) occurs via the uncommon phenomenon of single-file translation.¹²³ The study authors also suggest that this mechanism can only be observed by QENS, leading them to speculate that the popular hopping mechanism described in previous studies may be single-file diffusion that was mischaracterised by the chosen analytical method.

Clearly, QENS is a powerful technique that can yield key mechanistic insights into guest diffusion in MOFs. QENS is particularly useful in the analysis of proton conduction which we discuss at the end of this section.

Microimaging (IFM/IRM) (timescale: seconds to minutes)

Unlike QENS/PFG-NMR, microimaging by interference microscopy (IFM) or infrared microimaging (IRM) enables spatially-resolved visualisation of transient guest concentrations and guest fluxes, with time and space resolution of seconds and microns.¹²⁴⁻¹²⁷

IFM has primarily been used to study diffusion in zeolites,^{128,129} however in 2007 Kortunov demonstrated the first use of IFM for measuring guest diffusion in MOFs.¹³⁰ Since the refractive index of the crystal is proportional to changes in local concentration, recording interference patterns leads directly to guest concentration profiles. In this proof-of-concept study, it was found that diffusivity of methanol in a manganese formate MOF remained constant from no-loading to the pore-filled state.

In IRM, changes in local guest concentration are proportional to changes in characteristic IR bands of absorbing guest species and while the spatial resolution of IRM is less than that of IFM, it provides chemical information that allows simultaneous measurement of multiple species.¹³¹⁻¹³⁴ A growing number of examples have been reported of IRM used to study either gas sorption/release in MOF single crystals,¹³⁵⁻¹³⁷ or time-dependent drug release from MOFs.¹³⁸ Bux found that for streams of pure gasses (CO₂, CH₄) in ZIF-8, the host-guest and guest-guest interactions cause an increase in mobility at low loadings.¹³⁹ These increases disappear at high loadings or in a mixed gas stream, attributed to the steric effects of clustering and pore-window blocking. Contrary to the trends shown in methane and CO₂, diffusivity of alcohols initially decreases as loading rises from zero, as a result of hydrogen-bonded guest cluster-formation, until a minimum is reached. Beyond this loading, diffusivity then increases.

The IRM data from two related studies showed that ethane diffusion is faster than ethene in ZIF-11, despite ethane being smaller.^{140,141} It appears that ethene binds to ZIF-11 preventing linker rotation and restricting flexibility and pore aperture size, in an example where electronic effects and the consequent reduction in framework flexibility interact to increase the steric blocking of guest diffusion. In a related mixed-linker framework, ZIF-7-8, ethane diffusion is slower than in single-linker framework ZIF-7 due to a smaller pore aperture.¹⁴¹ Notably, across a single crystal of ZIF-7-8, a large range of diffusivities was observed. This is to be expected in mixed linker MOFs where the composition can vary across a material and this result showcases the benefits of non-spatially averaged data attained by IRM.

IFM and IRM provide a unique insight into guest diffusion in MOFs. In addition to the benefits described above, the transient concentration profiles obtained could be useful in tracking the formation of MOFs, where many different species are present.

QCM (timescale: seconds)

Changes in vibrational frequency of a piezoelectric quartz crystal under an applied AC current can be directly related to changes in mass on its surface. By virtue of this, quartz crystal microbalance (QCMs) have been used for decades as precise mass balances with nanogram sensitivity¹⁴²⁻¹⁴⁵ and have recently been employed with MOFs for high precision sensing.¹⁴⁶

Wöll *et al.* demonstrated that QCM could be used to study diffusion in MOFs in 2010.¹⁴⁷ They have since used this method to investigate cyclohexane uptake and diffusion in HKUST-1,¹⁴⁸ and ferrocene diffusion in MOF thin films.^{149,150} In the course of these studies they identified a rather elusive surface barrier effect which can hinder guest uptake in MOFs. They showed that surface barriers were caused by defects formed by exposure to air/humidity and found that these barriers can be removed by re-immersion in the synthesis solvent.¹⁵¹

QCM is a powerful technique that can elucidate guest loading, diffusion coefficients and mechanistic detail. The technique is underutilised in the field of MOFs and certainly deserves more recognition as an effective method for the study of guest motion.

Proton Conduction

The field of proton conducting materials is vast in its own right and the application of MOFs for these purposes has been extensively reviewed.¹⁵²⁻¹⁵⁴ As such, this section highlights just a handful of important cases whereby the motion of hydrogen nuclei has been revealed either via novel methods or where an unusual behaviour has been demonstrated. A wide variety of techniques can be employed to study motion of this kind, such as electrochemical Impedance Spectroscopy (EIS),¹⁵⁵ QENS and ²H solid state-NMR which help elucidate diffusivity and mechanistic information.^{156,157}

Proton conduction in MOFs usually occurs in one of two ways: a “Grotthuss” mechanism with $E_a < 0.4$ eV or by the vehicular mechanism where $E_a > 0.4$ eV.^{158,159} A 2016 study by Pili identified an alternative mechanism of proton conduction in MOF MFM-500(Ni).¹⁶⁰ QENS was used to elucidate the mechanism of proton motion as being “free diffusion inside a sphere”. The same mechanism was reported in 2019 in barium-based MOF, MFM-512.¹⁶¹ The framework contains free carboxylic acid groups which facilitate proton conduction via an extended hydrogen-bonded network with water. At 99% relative humidity the related MFM-511 had a proton conductivity of $5.1 \times 10^{-5} \text{ S cm}^{-1}$ while the free acid containing MFM-512 reported a conductivity of $2.9 \times 10^{-3} \text{ S cm}^{-1}$, showing the importance of free-acids in mediating moisture-induced proton conduction.

As well as needing high conduction, MOFs for applications in membrane materials for fuel cells¹⁶²⁻¹⁶⁴ and supercapacitors^{165,166} also require some form of control. Liang demonstrated proton conductivity modulation using light in SSP@ZIF-8 where SSP = sulfonated spiropyran.¹⁶⁷ The zwitterionic MC phase of SSP which predominates in the dark, forms a hydrogen-bond network throughout the structure which facilitates proton conduction (0.05 S cm^{-1} , just 4 times smaller than commercial standard Nafion at 0.2 S cm^{-1}). When exposed to visible light the SSP isomerises back to the neutral SP form, breaking the extended hydrogen bond network and reducing the conductivity by 28,000x. As well as the high on/off ratio, SSP@ZIF-8 boasts exceptional recyclability with stability over 100 cycles and a rapid response time of 5 seconds. Several other recent studies confirm the use of spiropyrans and other photoactive moieties embedded in MOFs to offer control over proton conductivity.¹⁶⁷⁻¹⁷⁰

Song reports a reversible amorphous-to-crystalline structure change in a magnesium formate ($\text{Mg}(\text{HCO}_2)_2$) MOF that is capable of on/off conductivity switching.¹⁷¹ The wet material is crystalline and has a proton conductivity of $1 \times 10^{-3} \text{ S cm}^{-1}$ but when the material dries it becomes amorphous and insulating. ²H NMR was used to study dynamics of proton transfer and characterise the mechanism as translational jump-diffusion of H_3O^+ molecules which are heavily restricted by the high activation barrier ($E_a = 0.58 \text{ eV}$).

In-situ crystallographic methods were employed by Wei to directly measure proton conductance.¹⁷² The MOF contained 2D europium-containing layers with phosphonium-based linkers connected by 1D Me_2NH_2^+ chains which point along the *c* direction. Single crystal AC impedance found that protons only conduct along this *c* direction, along the H-bond network. Variable-temperature single crystal X-ray diffraction (VT-SCXRD) combined with diffuse-reflectance infrared Fourier-transform spectroscopy (DRIFTS) analysis showed that at high temperatures, the bound proton of Me_2NH_2^+ moves closer to the phosphonium O^- . High enough temperatures caused protons to transfer from the Me_2NH_2^+ chains to the free phosphonate O^- giving rise to a new crystallographic phase due to evaporation of Me_2NH . The methods outlined in this work will greatly aid in the design and analysis of proton conducting MOFs in the future.

Protons are of course the smallest cations, but ion-conduction of larger ions in MOFs is also developing as a closely-related field. Lithium-ion conduction is of particular interest for emerging battery technologies for energy storage and, in 2018, Shen *et al.* described the decoration of open metal sites in MOFs with ClO_4^- ions, which afforded biomimetic lithium-ion channels with the ability to conduct Li^+ ions.¹⁷³ The highest conductivity was achieved by MIL-100(Al) which, after reacting with LiClO_4 , had a Li^+ conductivity of over 1 mS cm^{-1} , measured by EIS. In a direct comparison of MOFs UiO-66 and UiO-67, the latter displayed higher conductivity (0.65 vs 0.18 mS cm^{-1}) attributed to larger pores facilitating efficient solvation of Li^+ ions and reduced confinement effects.

Moving to even larger ions, ionic liquid (IL) conduction in MOFs is another developing area.^{174,175} Of particular relevance to this discussion is the example reported by Kanj *et al.* in 2019 wherein the authors investigated the loading-dependent ion conduction of ionic liquid 1-butyl-3-methylimidazolium bis(trifluoromethylsulfonyl)amide in framework HKUST-1.¹⁷⁶ Conventional fluids in nanoconfinement display their highest molecular transport rates at low loading when guest-guest interactions are minimal, with increased loading reducing transport rates as guest-guest interactions become dominant. The IL transport in HKUST-1 recorded by EIS displayed analogous behaviour with these two transport regimes until the highest loadings were reached when an unanticipated further significant drop in ion transport was observed. Molecular dynamics simulations enabled the authors to attribute this third transport regime to a new 'ion bunching' mechanism in which cations and anions mutually block pores and clog the conduction pathways.

Concluding Remarks

Several of the examples outlined above have used a combination of experiment and computation to understand guest diffusion, but the application of multiple experimental techniques to a single system is still very limited. No single technique can probe the entire timescale necessary to monitor non-uniform diffusion on the nano- to macro-scale, but employing multiple methods could bridge the gap. For example, QCM could be used to interrogate the initial sorption kinetics and possible surface barriers of guest uptake into a "bulk" MOF sample. The direct nature of the QCM mass measurement provides the necessary time resolution to monitor mass changes in seconds, but the slower-to-perform PFG-NMR or QENS experiments would then be a better choice to inform on fast guest diffusion within the body of the MOF. This is an example of how the time taken to measure a process is not the same as the time-dependence of the process measured, highlighting the difference between measuring non-equilibrium dynamic processes (gas uptake) and equilibrium situations (fixed loading, rapid guest diffusion on ns-ms timescales) respectively. Furthermore, it is important to consider the sample form. PFG-NMR, QENS, in situ FTIR and QCM typically measure diffusion on bulk samples, such as powders or pressed pellets, while IFM and IRM study single crystals. Both instances have merit and provide complementary but different information. It is therefore advantageous to develop methods that permit the use of a technique on bulk material and individual crystallites, but since this is often difficult to achieve, again we encourage the combinational use of techniques can that probe guest behaviours on both many-particle samples and individual crystals.

We finished this section by looking at proton and ion transport. One of the major applications of proton-conductive materials is in proton-exchange membrane fuel cells (PEMFCs) where protons are used to counterbalance the flow of electrons and maintain charge neutrality. In the next section we therefore turn our attention to electron motion within MOFs.

Electron motion

Chemistry is, at the most fundamental level, described by the behaviour of electrons. In this section we focus on the motion of electrons in MOFs, considering specifically that which is important to charge-transfer processes. The vast majority of MOFs are not electrically conductive, however if the orbital overlap is favourable, electrons are able to flow through a framework. We review techniques that measure electron transfer processes within MOFs, providing insights into photoconductivity, excited state dynamics and charge-transfer (Figure 4). Such information underpins development of electroactive MOFs for use as electrocatalysts,¹⁷⁷⁻¹⁸⁰ rechargeable batteries/supercapacitors^{166,181-184} and conductive membranes in fuel cells.^{97,185-187} Furthermore, the tuneable and often crystalline nature of MOFs makes them ideal media for investigating the fundamental principles governing the flow of charge in three-dimensional coordination space.¹⁸⁸

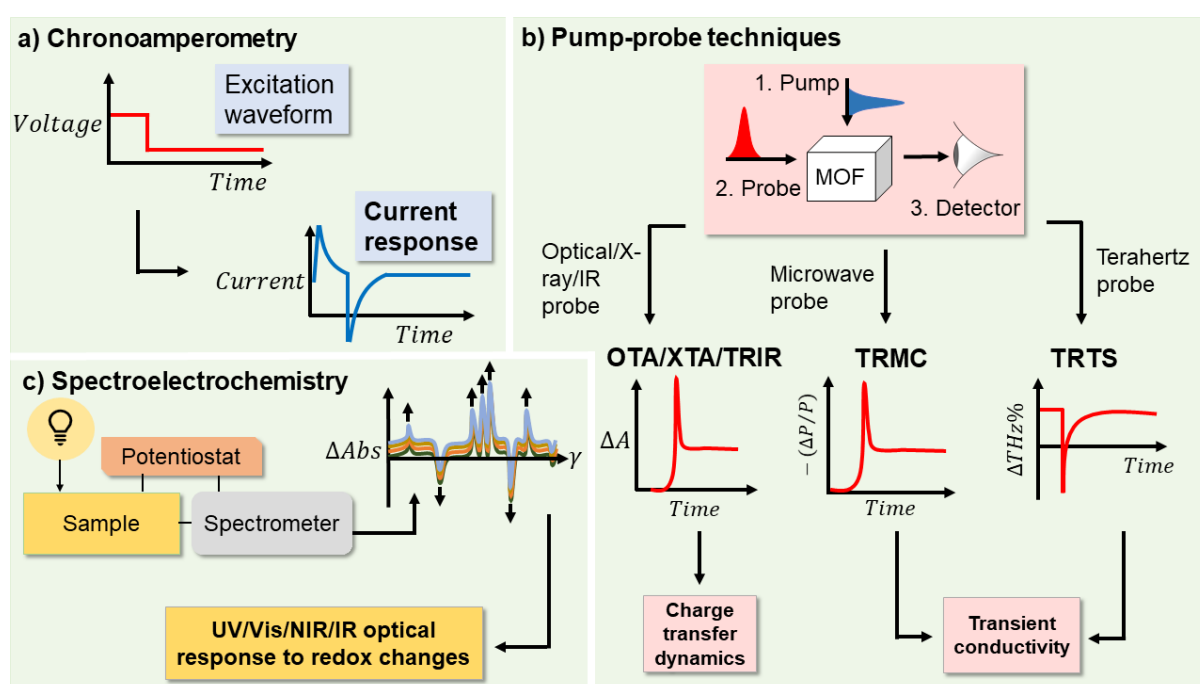


Figure 4. Experimental methods to probe electron motion in MOFs. a) Chronoamperometry monitors current response of a framework to an applied bias as a function of time; b) pump-probe techniques time-resolved terahertz spectroscopy (TRTS) and time-resolved microwave conductivity (TRMC) monitor photoconductivity on sub-picosecond timescales, and optical transient absorption/X-ray transient absorption/time-resolved infrared spectroscopy (OTA/XTA/TRIR) can all probe charge transfer and excited state dynamics; c) Spectroelectrochemistry (SEC) synchronises optical spectroscopic response with redox changes.

Transient spectroscopy (timescale: femtoseconds)

Characterising the excited states of electroactive MOFs is necessary for realising their applications in solar cells,¹⁸⁹ fuel cells and artificial photosynthesis.¹⁹⁰ Pump-probe experiments are well-established in the study of excited-state dynamics^{191,192} in gas, solution and solid-states,¹⁹³⁻¹⁹⁶ and typically proceed by exciting the system and then probing the transiently populated excited states using ultra-fast laser set-ups.

Optical transient absorption (OTA) and X-ray transient absorption (XTA) are pump-probe techniques that differ only in the wavelength of the “probe”. Pattengale *et al.* explored the excited state and

charge separation dynamics of ZIF-67 (Co²⁺) thin-films using both techniques.¹⁹⁷ OTA revealed the relaxation dynamics of an exceptionally long-lived excited state ($\tau = 2.9 \mu\text{s}$) formed after photoexcitation of the spin-allowed d-d transition of Co²⁺ ion in ZIF-67, shown by XTA to result from a ps-timescale Co²⁺ to Co⁺ reduction upon photoexcitation. The same group also demonstrated direct node-to-node communication in ZIF-67 (Co²⁺) partially transmetalated with either Zn²⁺ or Cu²⁺ ions.¹⁹⁸ Incorporation of closed shell Zn²⁺ into ZIF-67 impeded the formation of the excited charge separated state, characterised by OTA, but incorporation of redox active Cu²⁺ facilitated charge transport from excited Co²⁺ to Cu²⁺ centres, readily characterised by XTA. Being able to directly probe charge transfer processes not only offers mechanistic insight necessary for photoenergy applications but also neatly demonstrates how to spectroscopically interrogate MOFs in a way that underscores the advantages of combining multiple techniques.

These are challenging experiments. Hanna *et al.* tried employing the same combination of techniques to study photoexcitation of a ligand-to-metal charge transfer (LMCT) state in oleylamine-stabilised nanoparticles of MIL-100(Fe).¹⁹⁹ Scattering effects of the MOF colloidal suspension resulted in a weak OTA signal but XTA was able to show that the lifetime of this LMCT state was approximately three orders of magnitude longer than that measured by OTA for a molecular reference complex.

When appropriately emissive components are present, ultrafast transient emission spectroscopy can also provide dynamic insight into excited-state electron-transfer processes in MOFs, especially when coupled with ultrafast OTA measurements. Yu *et al.* investigated the excited states of compositionally identical but topologically different pyrene-containing MOFs NU-901 and NU-1000.²⁰⁰ From the solvent-dependent ps-timescale transient fluorescence spectra, low-lying polar excitonic states were shown to influence the excited-state population decay process in NU-1000 more than NU-901 because of their distinct topologies. Porphyrin-based Zn-SURMOFs were studied by Li *et al.* who were able to observe subpicosecond and picosecond S₂-S₁ internal conversion and decay processes, with strong quenching of both states when compared with molecular analogue Zn(TPP) (TPP = tetraphenylporphyrin) in ethanol.²⁰¹ This quenching was attributed to efficient energy transfer between adjacent chromophores in the MOF environment and is a function of the spatial preorganisation that the framework provides.

By immobilising M(2,2'-bipyridine)(CO)₃X moieties (where M = Re or Mn, and X = Cl or Br) within MOFs, Blake *et al.* were able to study the excited state dynamics of Re(diamine)CO₃Cl complexes in 3D coordination space using time-resolved infrared spectroscopy (TRIR).¹⁹⁵ Such complexes have been widely studied in solution for their potential photocatalytic applications and typically the lowest-energy longest-lived excited state is the solvent-stabilised ³MLCT state.²⁰² However, TRIR spectra of the pressed MOF powder sample showed that while both ³MLCT and $\pi\text{-}\pi^*$ states were formed by initial photoexcitation the ³MLCT bands decayed surprisingly rapidly ($\tau = 20 \text{ ps}$) and the ³ $\pi\text{-}\pi^*$ state had a much slower decay lifetime ($\tau = \sim 23 \text{ ns}$) before reforming the parent species. By isolating the photoactive Re complex in a MOF, no solvent-stabilisation effects or intermolecular $\pi\text{-}\pi$ stacking were possible and thus the authors were able to directly observe interconversion of the ³MLCT excited state into the $\pi\text{-}\pi^*$ state and reversal of the energy ordering of these states.

In a related study, Eason *et al.* investigated the photoinduced charge-transfer process occurring in mixed metal framework, ReCu ((Cu(DMF)(H₂O)[LRe(CO)₃Cl])·DMF)_∞.¹⁹⁶ The pressed pellet TRIR spectrum again showed initial formation of a ³MLCT state. Temporal investigation revealed rapid decay to an intraligand ³ $\pi\text{-}\pi^*$ state (lifetime = $102 \pm 15 \text{ ps}$) with concurrent partial reformation of the ground state (lifetime = $105 \pm 10 \text{ ps}$). However, an additional longer-range low quantum-yield irreversible charge-transfer process that reduced the Cu²⁺ nodes was also identified in the data.

Exploiting this, the authors demonstrated spatially-resolved modification of the ReCu crystal using focused laser irradiation to 'write' on single crystals.

In-situ spectroelectrochemistry (in-situ SEC) (timescale: seconds)

Continuing the spectroscopic theme, but moving to a much longer timescale, *in-situ* spectroelectrochemistry (SEC) describes the combined usage of spectroscopic and electrochemical techniques to follow redox processes.²⁰³ The technique requires specially designed electrochemical cells which permit probing of intermediate species through spectroscopic techniques like Raman, electron paramagnetic resonance (EPR), and ultraviolet/visible/near-infrared absorption spectroscopy (UV/vis/NIR).

Using a combination of *in-situ* SEC techniques (UV/vis/NIR, EPR), Hua *et al.* identified that reduction of MOF $[\text{Zn}_2(\text{BPPTzTz})_2(\text{tdc})_2]_n$ (BPPTzTz = 2,5-bis(4-(pyridine-4-yl)phenyl)thiazolo[5,4-d]thiazole, tdc = 2,5-thiophenedicarboxylate) formed a mixed-valence state with an inter-valence charge-transfer (IVCT) occurring over 3.80 Å between cofacial thiazolo[5,4-d]thiazole moieties.²⁰⁴ The very closely-related IVCT in reduced forms of isotopological frameworks $[\text{Zn}_2(\text{BDPPTzTz})_2(\text{SDC})_2]$ and $[\text{Cd}_2(\text{BDPPTzTz})_2(\text{SDC})_2]$ (SDC = selenophene-2,5-dicarboxylate) were similarly investigated by Ding *et al.*, who also used *in-situ* EPR and vis-NIR SEC.²⁰⁵ The electron mobility of the Cd(II) analogue was around 3x smaller than that of the Zn(II) MOF because the larger size of the Cd(II) ions resulted in poorer band overlap between ligand pairs.

In-situ Raman SEC was used in 2018 by Usov *et al.* to monitor the redox-dependent and pressure-dependent charge-transfer properties of donor-acceptor MOF $[(\text{Zn}(\text{DMF}))_2(\text{TTFTC})(\text{DPNI})]$ (TTFTC = tetrathiafulvalene tetracarboxylate, DPNI = N,N'-di(4-pyridyl)-1,4,5,8-naphthalenetetracarboxydiimide).²⁰⁶ They identified the formation of a new electrochemically-generated radical cationic complex in which charge-transfer is heterogeneously distributed throughout the framework. Notably, they also employed 2-point probe conductivity to study the bulk pressed-pellet conductivity of this particularly interesting MOF, a property that in itself is of rising interest in the MOF community.

Flipping SEC on its head and using light as stimulus rather than probe, Garg *et al.* were able to demonstrate light-induced enhancement of electronic conductivity of a spiropyran-loaded UiO-67 MOF thin-film by one order of magnitude, measured by simple DC conductivity and thermally reversible at room temperature.²⁰⁷ Other photoswitches have also been used to impart conductivity control in framework materials, with Yu *et al.* notably reporting a dithienylethene-modified covalent organic framework film capable of switching on and off an LED in a circuit with the film simply by alternating between UV and visible light irradiation.²⁰⁸ Light-induced changes in film conductivity were characterised by a combination of optical spectroscopies and conductivity measurements. The interrogation of sample conductivity can be challenging, and hence we discuss promising time-dependent methods next.

Conductivity measurement: TRMC and TRTS (timescale: femtoseconds to nanoseconds)

Measuring conductivity of solid samples can be done either in bulk (typically a pressed pellet) or on a single crystal. EIS can be used to measure conductivity,¹⁵⁵ however the measured value is strongly dependent on the type of contact method (e.g., direct contact, wire-paste, *in-situ* press or probe-paste methods) and can result in discrepancies of up to 2 orders of magnitude.²⁰⁹

An alternative is to use non-contact methods, such as time-resolved microwave conductivity (TRMC) which measures conductivity as a function of time (down to ns time resolution) without electrically contacting the sample. Free electrons absorb microwaves so changes in the conductivity of a

materials can be obtained by changes in transmitted microwave power. Narayan *et al.* used TRMC to measure the transient conductivity of semi-conductive MOF, $\text{Zn}_2(\text{TTFTB})$ (TTFTB = tetrathiafulvalene tetrabenzoate), which was in turn used to calculate its intrinsic charge mobility ($0.2 \text{ cm}^2 / \text{Vs}$).²¹⁰ Later, Aubrey *et al.* used TRMC to study electron delocalisation and charge mobility as a function of reduction in $\text{K}_x\text{Fe}_2(\text{BDP})_3$ ($0 \leq x \leq 2$) (BDP = 1,4-benzenedipyrazolate).²¹¹ The study showed that fractional reduction of the MOF increased conductivity along one direction 10,000-fold.

A similar technique, time-resolved terahertz spectroscopy (TRTS), measures transient conductivity by detecting changes in THz transmittance and has increased time resolution (ps) due to its higher frequency and shorter response times. Dong *et al.* investigated the conductivity and charge transport mechanism of a semiconducting pi-d conjugated MOF, $\text{Fe}_3(\text{THT})_2(\text{NH}_4)_3$ (THT = 2,3,6,7,10,11-hexathioltriphenylene).²¹² TRTS measurements revealed the nature of charge-transport as being Drude-type, which was subsequently corroborated by Hall-effect measurements.

TRMC and TRTS have no grain boundary effects or random orientation effects that plague contact methods, and there are no anisotropy issues. The field is in need of a standardised method for measuring local conductivity and TRMC and TRTS may offer the solution.

Chronoamperometry (timescale: milliseconds)

Electron and ion diffusion on the ms timescale can be studied by chronoamperometry, a time-dependent electrochemical technique which measures a current vs time response. In 2020, Cai *et al.* used chronoamperometry to independently measured the ion and electron diffusivities in ferrocene-doped MOFs of increasing pore sizes (MOF-808, NU-1000 and NU-1003), finding that electron diffusivity decreased while ion diffusivity increased to a greater extent.²¹³ This meant overall charge diffusivity increased with increasing pore size, ultimately being limited by ion diffusion.

Concluding remarks

The *in-situ* and time-resolved measurement of electron motion within MOFs represents a key tool for the elucidation of MOF electronic structure and function. Understanding charge transfer mechanisms, excited state dynamics and photoconductivity are essential for the design of electroactive MOFs for use in electrochemical applications. As with the study of MOF formation, a combined approach is again desirable to obtain as full a picture as possible, choosing complementary techniques for the specific length- and time-scales they are capable of probing. Technological advances mean there are numerous opportunities for new combinations of methods to be developed that span greater time and length scales.

Framework motion

Introduction

In this final section, we look at the various techniques that are able to directly measure motion of framework structural components. MOF flexibility is a hot topic in the field and has been reviewed by others recently, primarily from framework perspectives.^{7,214-216} Many of the potential applications of dynamic MOFs rely on understanding how framework properties change after an applied stimulus. There are many types of framework motion, for example gate-opening, SC-SC transitions, breathing, and swelling.²¹⁷⁻²²⁰ Here we describe several time-resolved/*in-situ* techniques (Figure 5)

capable of probing these phenomena after application of stimuli including changes in guest adsorption, temperature, pressure, and light.

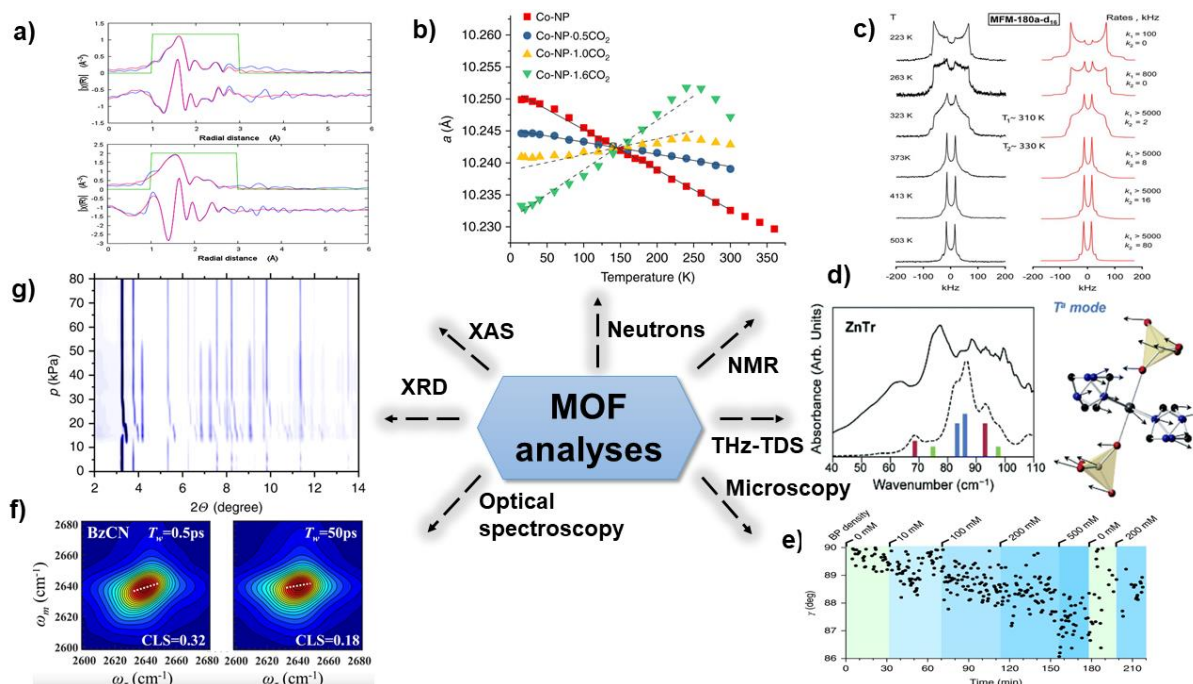


Figure 5. A selection of works from the literature highlighting the wealth of information gained from utilizing the *in-situ* techniques discussed in this section of the review. a) extended X-ray absorption fine structure (EXAFS) data analysis showing a unique deformation in the nickel-based paddle-wheel node of DUT-8(Ni) before and after N_2 adsorption²⁴⁹; b) negative-to-positive tuning of the thermal expansion coefficient of MOF Co-NP due as a function of CO_2 uptake²⁴²; c) 2H solid-state NMR spectroscopy revealing the reorientation mechanisms within octacarboxylate MOF MFM-180; d) terahertz time-domain spectroscopy (THz-TDS) spectrum revealing collective vibrational modes responsible for the proton conductivity of MOF ZnTr; e) LP-AFM data showing a reversible change in framework surface structure from a tetragonal unit cell to rhombic as a function of guest concentration; f) two-dimensional infrared spectroscopy (2D IR) spectra of deuterated bridging hydroxyl (μ_2 -OD) in MIL-53(Al) loaded with BzCN at $T_w = 0.5$ ps and $T_w = 50$ ps from which information regarding the hydrogen bonding dynamics can be extracted; g) *in-situ* powder X-ray diffraction (PXRD) contour plot of pressure-amplifying framework DUT-49 during N_2 adsorption.

In-situ XRD (timescale: seconds to hours)

Since most MOFs are crystalline, time-resolved and *in-situ* X-ray diffraction methods are often the method of choice for gaining structural insight into a dynamic event such as a phase transition or distortion. Burtch *et al.* employed *in-situ* powder X-ray diffraction (PXRD) to study $Zn_2(BDC-TM)_2(DABCO)$ ($BDC-TM = 2,3,5,6$ -tetramethyl-1,4-benzenedicarboxylic acid, $DABCO = 1,4$ -diazabicyclo[2.2.2]octane), which undergoes a reversible domino-lattice rearrangement on water sorption.²²¹ The findings showed that even MOFs which retain their crystallinity and porosity upon moisture exposure can undergo significant molecular-level structural change due to guest-host interactions. Similarly, Lo *et al.*, utilised *in-situ* PXRD to track a desolvation-triggered domino-lattice rearrangement in AlTz-53.²²² Within 40 s of activation, AlTz-53 undergoes a reversible phase transition from a disordered, low porosity state (interconnected sql nets) to a highly crystalline one with high porosity (interconnected kgm nets). This transition between distinct topological states was shown to be reversible over 4 cycles through activation and re-immersion in polar solvents.

Through an arsenal of experimental and computation techniques Krause *et al.* were able to unpick several factors affecting the probability of a MOF exhibiting negative gas adsorption (NGA): linker length, interpenetration, framework softness and mechanical stiffness.²²³ *In-situ* PXRD was used to analyse the micromechanical properties of the isoreticular MOFs DUT-46, DUT-48, DUT-49, DUT-50 and DUT-151 upon adsorption of guests. The authors discovered a new pressure-amplifying framework in DUT-50, with even higher pore volume and pore size than DUT-49 and later reported that crystallite size has a pronounced effect on the NGA behaviour of DUT-49.²²⁴

The nature of the solvent-switchable continuous breathing mechanism of structure change in SHF-61 was investigated by Carrington *et al.* by means of *in-situ* PXRD.²²⁵ Continuous breathing differs from traditional breathing behaviour in that no phase transition appears to occur. In SHF-61 the mechanism was found to be highly guest dependent. This offers the possibility to control guest uptake and selectivity; they elegantly demonstrated that gated CO₂ uptake could be achieved by partially solvating with DMF.

Some MOFs display negative linear compressibility (NLC) whereby contraction in one direction under hydrostatic pressure is accompanied by elongation in one or more directions.²²⁶⁻²²⁸ Cai *et al.* demonstrated a temperature-induced positive correlation between NLC and positive thermal expansion (PTE) with the MOF [Ag(ethylenediamine)]NO₃.²²⁹ Using variable-temperature and variable-pressure *in-situ* SCXRD, the mechanism for this direct coupling between NLC and PTE is presented as resulting from the voids “inflating” and the framework “scissors-opening” motion.

It should be noted that *in-situ* measurements are not “time-resolved” if patterns are recorded at equilibrated pressures. There is an opportunity to gain more information by conducting true time-resolved measurements at non-equilibrated pressures. New detector technologies, such as Hybrid Pixel Array detectors in use at the Diamond Light Source can improve acquisition time of XRD patterns, enabling truly time-resolved XRD experiments.^{230,231}

An inherent disadvantage of *in-situ* XRD for the study of framework motion is the inability to resolve any transient non-crystalline states traversed during a given phase transition. Developments in pair-distribution function capabilities and analyses, like those discussed in the framework synthesis section above, have also been applied to framework characterisation under dynamic stimuli. This area has been expertly reviewed in 2020 by Platero-Prats *et al.*²³² Returning to the limitations of more common and accessible X-ray diffraction methods, however, it is fair to say that XRD studies often parallelise their experiments with complementary spectroscopic or microscopic experiments, discussed in the next section.

In-situ optical and vibrational spectroscopies (timescale: milliseconds to minutes)

Optical and vibrational spectroscopies enable acquisition of molecular-level information on MOF dynamics without requiring crystallinity.⁸ Mao *et al.* studied the stability of magnesium formate MOF, Mg₃(HCOO)₆, as a function of hydrostatic pressure using *in-situ* Raman and *in-situ* FTIR.²³³ They found that the activated framework was stable up to a pressure of 2 GPa whereupon a SC-SC transition occurs. When the MOF was loaded with guests such as DMF or benzene, no SC-SC transition occurred. Extending further into the IR when examining framework structure change, Ryder *et al.* investigated the thermally induced amorphization of ZIF-4 and subsequent recrystallisation to ZIF-zni via *in-situ* synchrotron far-infrared (FIR) spectroscopy.²³⁴ By monitoring the vibrational changes of the ZnN₄ tetrahedra the authors could predict the likelihood of thermal-induced amorphization of a given ZIF.

Functionalisation of UiO-66 with a vibrationally active probe and subsequent two-dimensional infrared spectroscopy (2D-IR) spectroscopic analysis can yield information on ultrafast framework

dynamics, measuring the MOF structural elasticity.²³⁵ Framework deformations with time constants of 7 ps and 670 ps were identified, with the MOF structural dynamics slowing substantially when DMF was introduced to the framework. The same group used pump-probe femtosecond FTIR and 2D-IR to investigate local hydrogen-bonding dynamics as well as framework dynamics of MIL-53(Ni) loaded with benzonitrile, benzene, cyclohexane and phenyl selenocyanate.²³⁶ 2D-IR allows for the correlation of ultrafast changes in the hydrogen-bond with (i) dynamics of the hydrogen bond itself (sub-ps), (ii) framework dynamics (ps) and (iii) guest motion (>ns).²³⁷

Structural photoresponsivity in MOFs has been reviewed a number of times in past years^{32,238,239} so we provide only a few examples in this section. Azobenzene moieties are archetypal photoactive components and Mutruc *et al.* showed that a functionalised “shell” containing these molecules on the surface of UiO-68 permits light-gated guest diffusion.²⁴⁰ *In-situ* UV/vis diffuse reflectance spectroscopy showed an 86% increase in 1-pyrenecarboxylic acid uptake when in the “open” form (E-azobenzene) compared to when in the “closed” form (Z-azobenzene). Later, Liu *et al.* showed that a MOF membrane with photoactive azobenzene and bis(4-pyridyl)ethylene groups directly incorporated into the struts allowed reversible modulation of the separation factors of gas mixtures.²⁴¹ *In-situ* UV/vis spectroscopy showed that the separation factor of a H₂/CO₂ mixture could be reversibly switched between 21.3 and 43.7 due to reduced CO₂ adsorption when in the E-azobenzene state. Wang *et al.* have also demonstrated the ability to measure transient isomerisation of azobenzene within a MOF membrane using *in-situ* FTIR.²⁴² Spiropyran, another common photoactive component, have also been investigated in MOFs, albeit only as guests or pendent groups to either nodes or linkers and not with the spiro-core as an intrinsic part of the bridge between nodes.^{4,5,207} Williams *et al.* showed that the photoisomerization rates of MOFs functionalised with coordinatively immobilised spiropyran moieties grafted onto the sides of linkers could be modulated as a function of the framework structure to achieve completed photoconversion and photoisomerization rates comparable to free spiropyran in solution.²⁴³

Nuclear Magnetic Resonance (timescale: seconds to minutes)

In-situ ¹²⁹Xe NMR was used by Hoffmann *et al.* to investigate “gate opening” in DUT-8(Ni).²⁴⁴ The pore-opening of DUT-8(Ni) was characterised by a ¹²⁹Xe NMR signal with a chemical shift in the range 225-230 ppm, which exceeds that of liquid Xe outside the crystallites. ¹²⁹Xe NMR was also used to study the structure transition in pressure-amplifying DUT-49.²⁴⁵ The transition was observed at around 0.15 bar at 200 K by an increase in ¹²⁹Xe chemical shift from 130 to 230 ppm. This is indicative of increased wall-Xe interactions in the new closed-pore state. Additionally, coexistence of open-pore and closed-pore peaks at 0.66-0.88 bar suggests that the transition is a collective phenomenon taking place in larger domains/crystallites. A series of isoreticular DUT-49 MOFs were investigated using the same technique.²⁴⁶ Using the difference between the chemical shift of the adsorbed Xe and the chemical shift of bulk liquid Xe, the authors could estimate the mean pore size of these isoreticular MOFs.

In-situ ¹³C NMR is frequently used to investigate framework motion induced by carbon-containing guests such as CO₂ or hydrocarbons.²⁴⁷⁻²⁵¹ Sin *et al.* investigated the effect of framework flexibility of the uptake selectivity of CO₂ from a CO₂/CH₄ mixture.²⁵² Selectivity factors were calculated based on shift ratios; DUT-8(Ni)_flex is more selective than DUT-8(Ni)_rigid suggesting flexibility-enhanced selectivity.

Neutron studies (timescale: picoseconds to minutes)

Inelastic neutron scattering (INS) and quasi-elastic neutron scattering (QENS) are primarily used to study guest binding and motion within MOFs.²⁵³⁻²⁵⁵ However, cooperative effects can give insight into the motion of the framework surrounding the guests.²⁵⁶

Zhao *et al.* used QENS to determine the transport- and self-diffusivity of CO₂ in ZIF-7 at a loading of 1.3 mmol g⁻¹ at 298 K and 225 K.²⁵⁷ This data, in parallel with *in-situ* SCXRD and uptake isotherms showed how ZIF-7 undergoes a CO₂-induced structural change due to migration of CO₂ in its non-uniform pores rather than by the typical “gate-opening” adsorption mechanism. Another key technique is neutron powder diffraction (NPD). A major advantage of NPD over X-ray diffraction techniques is that both ¹H and ²H are strong scatterers of neutrons meaning their position and thermal motion can be more readily determined. Auckett *et al.* used NPD to monitor a phase transition occurring in two Prussian blue derivative frameworks.²⁵⁸ By varying the concentration of adsorbed CO₂, the thermal expansion coefficients of both frameworks were continuously and reversibly tuned from negative to positive values. These temperature-dependent NPD experiments are not time-resolved, as the temperature is equilibrated prior to recording each pattern, but the information obtained can shed light on time-dependent processes.

Microscopy (timescale: seconds to minutes)

As well as finding extensive use in the *in-situ* investigation of MOF synthesis, *in-situ* microscopy techniques have been proven to be effective time-resolved probes of framework dynamics.²⁵⁹ Hosono *et al.* studied local surface changes in MOFs during guest absorption in real time using LP-AFM.²⁶⁰ The surface was found to be highly guest-responsive, deforming on a timescale of 10 min in response to changes in guest concentration while the bulk crystal showed no lattice changes. This increased flexibility at the surface is speculated to be due to dynamic coordination binding at the solid-liquid interface as well as host-guest interactions, which has both practical and conceptual overlap with both the above-mentioned surface growth mechanisms identified by Zheng *et al.*⁶² and the surface defect ‘healing’ studied using QCM experiments and described by Wöll and co-workers.¹⁵¹

The moisture/temperature-induced breathing behaviour of individual MIL-53(Cr) nanocrystals was monitored directly by Parent *et al.* using environmental transmission electron microscopy (TEM) and computer simulations.²⁶¹ The breathing transition between 1 and 25 H₂O molecules is reversible by heating-cooling cycling. Environmental TEM (ETEM) is an effective method for studying framework-level changes occurring in individual MOF crystallites.

In recent years, microscopy techniques have proven themselves a valuable *in-situ* characterisation tool but their use in studying framework motion is uncommon compared to other techniques like XRD, NMR. The information gained from ETEM and LP-AFM is complementary to more traditional techniques and there is great scope for more in-depth study of framework dynamics.

XAS (timescale: minutes)

Many studies have demonstrated the utility of X-ray absorption spectroscopy (XAS) to gain local-structural information on the metal nodes in MOFs,^{262,263} but its use *in-situ* during structure changes is limited to a handful of examples. Kortright *et al.* used *in-situ* XAS to study the local electron structure around Cu²⁺ in Cu(dpa)₂SiF₆-i (dpa = dipyrityl acetylene) as a function of CO₂ uptake.²⁶⁴ Cu L_{2,3} edge spectra show weak systematic CO₂-induced effects resulting from distortions of the Cu²⁺ coordination shell.

Bon *et al.* went a step further and used *in-situ* extended X-ray absorption fine structure (EXAFS) to monitor the guest-induced phase transition in DUT-8(Ni).²⁶⁵ By monitoring changes in the EXAFS spectra during N₂ adsorption, node geometry changes were monitored during the closed phase → open phase transition. While this study looks at the distinct closed and open states without taking measurements during the transition (i.e. it has low time resolution) the technique is able to elucidate a unique local deformation of the nickel-based paddle-wheel node occurring between the

end states. A key area of improvement for this technique is the time resolution, which in principle could be increased to at least to the level of QEXAFS (100s of seconds).^{87,88}

THz-TDS (timescale: picoseconds)

A technique deserving of more attention is terahertz time-domain spectroscopy (THz-TDS) which is used to measure the frequency of lattice vibrations in MOFs.²⁶⁶⁻²⁶⁹ These collective fluctuations become static transitions when enough energy is supplied to the system. Typically, a frequency reduction is observed upon approaching a structural transition, and analysis of the changes in these THz modes provides insights into the transformation mechanism.²⁷⁰ These “soft modes” have been shown both *in silico* and through experiment to dictate many of the dynamic features of MOFs such as proton conduction²⁷¹ and framework mechanochemical properties.²⁷²⁻²⁷⁷ This avenue of research is therefore of fundamental importance to the field of MOF dynamics in the future.

Concluding remarks

The study of the framework motion itself is essential for the design of stimuli-responsive MOFs for targeted applications. As we have highlighted in this section, there are several experimental techniques that can achieve this. Additionally, there is no lone technique that can provide all the information necessary to understand the long-range crystallographic structural changes as well as molecular level local changes. Therefore, a combined approach whereby several different techniques are used in parallel is most effective.

Conclusions and perspectives

In this review we have summarised time-resolved techniques that have been used to study dynamic behaviours in and of MOFs. We have particularly focussed on the utility of these techniques in the context of fundamental studies. Some approaches are more common than others, such as XRD, TEM/SEM/AFM and NMR. However, there are a number of methods that clearly warrant more investigation, including QCM for studying guest behaviours, dAR-SHS and CLASSIC NMR for the study of MOF formation, and TRTS and TRMC for the time-resolved study of transient conductivity.

After a busy period of framework discovery, followed by increasingly elaborate framework design, the past decade has seen an explosion in the number of stimuli-responsive, flexible MOFs. There holds much promise in these materials for future applications, but the time domain is the key to unlocking that promise. If these applications are to be realised, fundamental studies of time-resolved phenomena must be explored.²⁷⁸ The methods briefly described above represent the pioneers of such exploration.

While not directly discussed in this review, it is important that we acknowledge the critical role of computational chemistry methods in the future of the MOF time domain. Parallel development of computational methods is an integral part of the way forward and we therefore refer the reader to two excellent reviews by Fraux, Chibani and Coudert^{34,279} which summarise the state and challenges of modelling stimuli-responsive MOFs. An exciting new trend is the application of machine learning (ML) to understanding in the field. The utility of ML in predicting MOF synthesis conditions and MOF properties is the subject of several recent reviews.^{280,281} The synergistic relationship between

computational and experimental methods is essential for the development of the field just as, for example, time-dependent DFT has become vital to the interpretation of time-resolved spectroscopic experiments that underpin much of our current understanding of the well-established field of photocatalysis.^{282,283} To that end, we recommend a recent 2021 review in which Speybroeck and coworkers have elegantly summed up the state-of-the-art for modelling spatiotemporal processes in MOFs from subnanometre to micrometer scale; their work highlights the need for a good understanding of realistic operating conditions and their interplay with computational modelling.²⁸⁴

There is already a growing appreciation for the time-resolved investigation of MOFs, with the challenge having been expertly laid down by Kaskel et al. in 2020 to deliberately design so-called '4D-MOFs' with precisely engineered energy barriers between multiple states, and to significantly improve terminology in the field, both qualitatively and quantitatively.³⁸ We have set out in this review to describe and summarise the technical methods by which the challenge can be met and the information those methods can already provide. Given that dynamic phenomena in MOFs happen on timescales from femtoseconds to hours, and on length scales from atoms to engineering rigs, no single method or technique is going to comprehensively solve all the questions that arise. We return therefore to Figure 1, noting that 'slow and macroscopic' phenomenological analyses (e.g. nucleation and crystal growth in MOF formation, gas sorption dynamics, ion conductivity) are well-served by existing methods. The ultrafast phenomena (e.g. excited-state decay, photocatalysis, charge-transfer dynamics) are less thoroughly covered and remain primarily the domain of laser-driven pump-probe experiments. Similarly, phenomena that can be interrogated with truly atomic spatial resolution (e.g. surface rearrangement on guest sorption, crystal growth at surfaces) are fewer, being largely limited to 2D or surface-only experiments. The technical challenge is therefore to develop combinations of analyses or bring in new techniques to the field that can bridge the time and space divide. Methods employed in other fields such as tip-enhanced Raman spectroscopy (TERS)²⁸⁵ offer the possibility of combining atomic resolution with vibrational spectroscopy, and MOFs represent an ideal platform on which to push the current limits of such methods. We are also particularly excited to see how time-resolved experimental data will in future be combined with computational methods to understand, design and generate novel MOF structures with predictable stimuli-responsive behaviours that lead to currently inconceivable applications.

References

- 1 Horike, S., Umeyama, D. & Kitagawa, S. Ion Conductivity and Transport by Porous Coordination Polymers and Metal–Organic Frameworks. *Accounts of Chemical Research* **46**, 2376–2384, doi:10.1021/ar300291s (2013).
- 2 Bhardwaj, S. K. *et al.* An overview of different strategies to introduce conductivity in metal–organic frameworks and miscellaneous applications thereof. *Journal of Materials Chemistry A* **6**, 14992–15009, doi:10.1039/C8TA04220A (2018).
- 3 Heinke, L. Diffusion and photoswitching in nanoporous thin films of metal-organic frameworks. *Journal of Physics D: Applied Physics* **50**, 193004, doi:10.1088/1361-6463/aa65f8 (2017).
- 4 Rice, A. M. *et al.* Photophysics Modulation in Photoswitchable Metal–Organic Frameworks. *Chemical Reviews* **120**, 8790–8813, doi:10.1021/acs.chemrev.9b00350 (2020).
- 5 Dolgoplova, E. A., Rice, A. M., Martin, C. R. & Shustova, N. B. Photochemistry and photophysics of MOFs: steps towards MOF-based sensing enhancements. *Chemical Society Reviews* **47**, 4710–4728, doi:10.1039/C7CS00861A (2018).
- 6 Mazaj, M., Kaucic, V. & Logar, N. Z. Chemistry of Metal-organic Frameworks Monitored by Advanced X-ray Diffraction and Scattering Techniques. *Acta Chimica Slovenica* **63**, 440–458, doi:10.17344/acsi.2016.2610 (2016).
- 7 Lee, J. H., Jeoung, S., Chung, Y. G. & Moon, H. R. Elucidation of flexible metal-organic frameworks: Research progresses and recent developments. *Coordination Chemistry Reviews* **389**, 161–188, doi:10.1016/j.ccr.2019.03.008 (2019).
- 8 Hanna, L. & Lockard, J. V. From IR to x-rays: gaining molecular level insights on metal-organic frameworks through spectroscopy. *Journal of Physics-Condensed Matter* **31**, doi:10.1088/1361-648X/ab38da (2019).
- 9 Bon, V., Brunner, E., Poppl, A. & Kaskel, S. Unraveling Structure and Dynamics in Porous Frameworks via Advanced In Situ Characterization Techniques. *Advanced Functional Materials* **30**, doi:10.1002/adfm.201907847 (2020).
- 10 Groom, C. R., Bruno, I. J., Lightfoot, M. P. & Ward, S. C. The Cambridge Structural Database. *Acta Crystallographica Section B-Structural Science Crystal Engineering and Materials* **72**, 171–179, doi:10.1107/s2052520616003954 (2016).
- 11 Tansell, A. J., Jones, C. L. & Easun, T. L. MOF the beaten track: unusual structures and uncommon applications of metal-organic frameworks. *Chemistry Central Journal* **11**, doi:10.1186/s13065-017-0330-0 (2017).
- 12 Easun, T. L. & Nevin, A. C. in *Organometallic Chemistry: Volume 42* Vol. 42 54–79 (The Royal Society of Chemistry, 2019).
- 13 Easun, T. L., Moreau, F., Yan, Y., Yang, S. & Schröder, M. Structural and dynamic studies of substrate binding in porous metal–organic frameworks. *Chemical Society Reviews* **46**, 239–274, doi:10.1039/C6CS00603E (2017).
- 14 Lin, R. B., Xiang, S. C., Xing, H. B., Zhou, W. & Chen, B. L. Exploration of porous metal-organic frameworks for gas separation and purification. *Coordination Chemistry Reviews* **378**, 87–103, doi:10.1016/j.ccr.2017.09.027 (2019).
- 15 Kang, Z. X., Fan, L. L. & Sun, D. F. Recent advances and challenges of metal-organic framework membranes for gas separation. *Journal of Materials Chemistry A* **5**, 10073–10091, doi:10.1039/c7ta01142c (2017).
- 16 Ma, S. Q. & Zhou, H. C. Gas storage in porous metal-organic frameworks for clean energy applications. *Chemical Communications* **46**, 44–53, doi:10.1039/b916295j (2010).
- 17 Dhakshinamoorthy, A., Asiri, A. M. & Garcia, H. Metal-Organic Framework (MOF) Compounds: Photocatalysts for Redox Reactions and Solar Fuel Production. *Angewandte Chemie-International Edition* **55**, 5414–5445, doi:10.1002/anie.201505581 (2016).

- 18 Zhang, T. & Lin, W. B. Metal-organic frameworks for artificial photosynthesis and photocatalysis. *Chemical Society Reviews* **43**, 5982-5993, doi:10.1039/c4cs00103f (2014).
- 19 Sun, Y. J. *et al.* Metal-Organic Framework Nanocarriers for Drug Delivery in Biomedical Applications. *Nano-Micro Letters* **12**, doi:10.1007/s40820-020-00423-3 (2020).
- 20 Lazaro, I. A. & Forgan, R. S. Application of zirconium MOFs in drug delivery and biomedicine. *Coordination Chemistry Reviews* **380**, 230-259, doi:10.1016/j.ccr.2018.09.009 (2019).
- 21 Horcajada, P. *et al.* Metal-Organic Frameworks in Biomedicine. *Chemical Reviews* **112**, 1232-1268, doi:10.1021/cr200256v (2012).
- 22 Wang, L., Zheng, M. & Xie, Z. G. Nanoscale metal-organic frameworks for drug delivery: a conventional platform with new promise. *Journal of Materials Chemistry B* **6**, 707-717, doi:10.1039/c7tb02970e (2018).
- 23 Lustig, W. P. *et al.* Metal-organic frameworks: functional luminescent and photonic materials for sensing applications. *Chemical Society Reviews* **46**, 3242-3285, doi:10.1039/c6cs00930a (2017).
- 24 Osman, D. I. *et al.* Nucleic acids biosensors based on metal-organic framework (MOF): Paving the way to clinical laboratory diagnosis. *Biosensors & Bioelectronics* **141**, doi:10.1016/j.bios.2019.111451 (2019).
- 25 Koo, W. T., Jang, J. S. & Kim, I. D. Metal-Organic Frameworks for Chemiresistive Sensors. *Chem* **5**, 1938-1963, doi:10.1016/j.chempr.2019.04.013 (2019).
- 26 Wen, X. D., Zhang, Q. Q. & Guan, J. Q. Applications of metal-organic framework-derived materials in fuel cells and metal-air batteries. *Coordination Chemistry Reviews* **409**, doi:10.1016/j.ccr.2020.213214 (2020).
- 27 Yang, L., Zeng, X. F., Wang, W. C. & Cao, D. P. Recent Progress in MOF-Derived, Heteroatom-Doped Porous Carbons as Highly Efficient Electrocatalysts for Oxygen Reduction Reaction in Fuel Cells. *Advanced Functional Materials* **28**, doi:10.1002/adfm.201704537 (2018).
- 28 Horike, S., Shimomura, S. & Kitagawa, S. Soft porous crystals. *Nature Chemistry* **1**, 695-704, doi:10.1038/nchem.444 (2009).
- 29 Boutin, A. *et al.* Temperature-Induced Structural Transitions in the Gallium-Based MIL-53 Metal-Organic Framework. *Journal of Physical Chemistry C* **117**, 8180-8188, doi:10.1021/jp312179e (2013).
- 30 Spencer, E. C. *et al.* Pressure-Induced Bond Rearrangement and Reversible Phase Transformation in a Metal-Organic Framework. *Angewandte Chemie-International Edition* **53**, 5583-5586, doi:10.1002/anie.201310276 (2014).
- 31 Allendorf, M. D. *et al.* Guest-Induced Emergent Properties in Metal-Organic Frameworks. *Journal of Physical Chemistry Letters* **6**, 1182-1195, doi:10.1021/jz5026883 (2015).
- 32 Jones, C. L., Tansell, A. J. & Easun, T. L. The lighter side of MOFs: structurally photoresponsive metal-organic frameworks. *Journal of Materials Chemistry A* **4**, 6714-6723, doi:10.1039/c5ta09424k (2016).
- 33 Ehrling, S., Miura, H., Senkowska, I. & Kaskel, S. From Macro- to Nanoscale: Finite Size Effects on Metal-Organic Framework Switchability. *Trends in Chemistry* **3**, 291-304, doi:10.1016/j.trechm.2020.12.012 (2021).
- 34 Fraux, G. & Coudert, F. X. Recent advances in the computational chemistry of soft porous crystals. *Chemical Communications* **53**, 7211-7221, doi:10.1039/c7cc03306k (2017).
- 35 Goeminne, R., Krause, S., Kaskel, S., Verstraelen, T. & Evans, J. D. Charting the Complete Thermodynamic Landscape of Gas Adsorption for a Responsive Metal-Organic Framework. *Journal of the American Chemical Society* **143**, 4143-4147, doi:10.1021/jacs.1c00522 (2021).
- 36 Tiba, A., Tivanski, A. V. & MacGillivray, L. R. Size-Dependent Mechanical Properties of a Metal-Organic Framework: Increase in Flexibility of ZIF-8 by Crystal Downsizing. *Nano Letters* **19**, 6140-6143, doi:10.1021/acs.nanolett.9b02125 (2019).
- 37 Krause, S. *et al.* The impact of crystal size and temperature on the adsorption-induced flexibility of the Zr-based metal-organic framework DUT-98. *Beilstein Journal of Nanotechnology* **10**, 1737-1744, doi:10.3762/bjnano.10.169 (2019).

- 38 Evans, J. D., Bon, V., Senkovska, I., Lee, H. C. & Kaskel, S. Four-dimensional metal-organic frameworks. *Nature Communications* **11**, doi:10.1038/s41467-020-16527-8 (2020).
- 39 Laybourn, A. *et al.* Metal-organic frameworks in seconds via selective microwave heating. *Journal of Materials Chemistry A* **5**, 7333-7338, doi:10.1039/C7TA01493G (2017).
- 40 Stock, N. & Biswas, S. Synthesis of Metal-Organic Frameworks (MOFs): Routes to Various MOF Topologies, Morphologies, and Composites. *Chemical Reviews* **112**, 933-969, doi:10.1021/cr200304e (2012).
- 41 Marshall, C. R., Staudhammer, S. A. & Brozek, C. K. Size control over metal-organic framework porous nanocrystals. *Chemical Science* **10**, 9396-9408, doi:10.1039/c9sc03802g (2019).
- 42 Shearer, G. C. *et al.* Defect Engineering: Tuning the Porosity and Composition of the Metal-Organic Framework UiO-66 via Modulated Synthesis. *Chemistry of Materials* **28**, 3749-3761, doi:10.1021/acs.chemmater.6b00602 (2016).
- 43 Kang, X. C. *et al.* Integration of mesopores and crystal defects in metal-organic frameworks via templated electrosynthesis. *Nature Communications* **10**, doi:10.1038/s41467-019-12268-5 (2019).
- 44 Fang, Z. L., Bueken, B., De Vos, D. E. & Fischer, R. A. Defect-Engineered Metal-Organic Frameworks. *Angewandte Chemie-International Edition* **54**, 7234-7254, doi:10.1002/anie.201411540 (2015).
- 45 Bennett, T. D., Cheetham, A. K., Fuchs, A. H. & Coudert, F. X. Interplay between defects, disorder and flexibility in metal-organic frameworks. *Nature Chemistry* **9**, 11-16, doi:10.1038/nchem.2691 (2017).
- 46 Zacher, D., Schmid, R., Woll, C. & Fischer, R. A. Surface Chemistry of Metal-Organic Frameworks at the Liquid-Solid Interface. *Angewandte Chemie-International Edition* **50**, 176-199, doi:10.1002/anie.201002451 (2011).
- 47 Seetharaj, R., Vandana, P. V., Arya, P. & Mathew, S. Dependence of solvents, pH, molar ratio and temperature in tuning metal organic framework architecture. *Arabian Journal of Chemistry* **12**, 295-315, doi:10.1016/j.arabjc.2016.01.003 (2019).
- 48 Asghar, A. *et al.* Efficient electrochemical synthesis of a manganese-based metal-organic framework for H₂ and CO₂ uptake. *Green Chemistry* **23**, 1220-1227, doi:10.1039/D0GC03292A (2021).
- 49 Asghar, A., Iqbal, N., Noor, T., Ali, M. & Easun, T. L. Efficient One-Pot Synthesis of a Hexamethylenetetramine-Doped Cu-BDC Metal-Organic Framework with Enhanced CO₂ Adsorption. *Nanomaterials* **9**, doi:10.3390/nano9081063 (2019).
- 50 Asghar, A. *et al.* Ethylenediamine loading into a manganese-based metal-organic framework enhances water stability and carbon dioxide uptake of the framework. *Royal Society Open Science* **7**, doi:10.1098/rsos.191934 (2020).
- 51 Van Vleet, M. J., Weng, T. T., Li, X. Y. & Schmidt, J. R. In Situ, Time-Resolved, and Mechanistic Studies of Metal-Organic Framework Nucleation and Growth. *Chemical Reviews* **118**, 3681-3721, doi:10.1021/acs.chemrev.7b00582 (2018).
- 52 Khawam, A. & Flanagan, D. R. Solid-state kinetic models: Basics and mathematical fundamentals. *Journal of Physical Chemistry B* **110**, 17315-17328, doi:10.1021/jp062746a (2006).
- 53 Davies, A. T., Sankar, G., Catlow, C. R. A. & Clark, S. M. Following the crystallization of microporous solids using EDXRD techniques. *Journal of Physical Chemistry B* **101**, 10115-10120, doi:10.1021/jp972557f (1997).
- 54 Muncaster, G. *et al.* On the advantages of the use of the three-element detector system for measuring EDXRD patterns to follow the crystallisation of open-framework structures. *Physical Chemistry Chemical Physics* **2**, 3523-3527, doi:10.1039/b004171h (2000).
- 55 Wu, Y. *et al.* Time-Resolved InSitu X-ray Diffraction Reveals Metal-Dependent Metal-Organic Framework Formation. *Angewandte Chemie-International Edition* **55**, 14081-14084, doi:10.1002/anie.201608463 (2016).

- 56 Wu, Y., Moorhouse, S. J. & O'Hare, D. Time-Resolved in Situ Diffraction Reveals a Solid-State Rearrangement During Solvothermal MOF Synthesis. *Chemistry of Materials* **27**, 7236-7239, doi:10.1021/acs.chemmater.5b03085 (2015).
- 57 Wu, Y., Breeze, M. I., O'Hare, D. & Walton, R. I. High energy X-rays for following metal-organic framework formation: Identifying intermediates in interpenetrated MOF-5 crystallisation. *Microporous and Mesoporous Materials* **254**, 178-183, doi:10.1016/j.micromeso.2017.04.043 (2017).
- 58 Ragon, F. *et al.* In Situ Energy-Dispersive X-ray Diffraction for the Synthesis Optimization and Scale-up of the Porous Zirconium Terephthalate UiO-66. *Inorganic Chemistry* **53**, 2491-2500, doi:10.1021/ic402514n (2014).
- 59 Ragon, F., Chevreau, H., Devic, T., Serre, C. & Horcajada, P. Impact of the Nature of the Organic Spacer on the Crystallization Kinetics of UiO-66(Zr)-Type MOFs. *Chemistry-a European Journal* **21**, 7135-7143, doi:10.1002/chem.201406119 (2015).
- 60 Wells, S. A., Cessford, N. F., Seaton, N. A. & Duren, T. Early stages of phase selection in MOF formation observed in molecular Monte Carlo simulations. *Rsc Advances* **9**, 14382-14390, doi:10.1039/c9ra01504c (2019).
- 61 Mazaj, M. & Logar, N. Z. Phase Formation Study of Ca-Terephthalate MOF-Type Materials. *Crystal Growth & Design* **15**, 617-624, doi:10.1021/cg501273b (2015).
- 62 Zheng, C. M., Greer, H. F., Chianga, C. Y. & Zhou, W. Z. Microstructural study of the formation mechanism of metal-organic framework MOF-5. *Crystengcomm* **16**, 1064-1070, doi:10.1039/c3ce41291a (2014).
- 63 Yeung, H. H. M. *et al.* InSitu Observation of Successive Crystallizations and Metastable Intermediates in the Formation of Metal-Organic Frameworks. *Angewandte Chemie-International Edition* **55**, 2012-2016, doi:10.1002/anie.201508763 (2016).
- 64 Yeung, H. H. M. *et al.* Control of Metal-Organic Framework Crystallization by Metastable Intermediate Pre-equilibrium Species. *Angewandte Chemie-International Edition* **58**, 566-571, doi:10.1002/anie.201810039 (2019).
- 65 Boldon, L., Laliberte, F. & Liu, L. Review of the fundamental theories behind small angle X-ray scattering, molecular dynamics simulations, and relevant integrated application. *Nano Reviews & Experiments* **6**, doi:10.3402/nano.v6.25661 (2015).
- 66 Narayanan, T. *et al.* A multipurpose instrument for time-resolved ultra-small-angle and coherent X-ray scattering. *Journal of Applied Crystallography* **51**, 1511-1524, doi:10.1107/s1600576718012748 (2018).
- 67 Carraro, F. *et al.* Continuous-Flow Synthesis of ZIF-8 Biocomposites with Tunable Particle Size. *Angewandte Chemie-International Edition* **59**, 8123-8127, doi:10.1002/anie.202000678 (2020).
- 68 Cravillon, J. *et al.* Fast Nucleation and Growth of ZIF-8 Nanocrystals Monitored by Time-Resolved In Situ Small-Angle and Wide-Angle X-Ray Scattering. *Angewandte Chemie-International Edition* **50**, 8067-8071, doi:10.1002/anie.201102071 (2011).
- 69 Stavitski, E. *et al.* Kinetic Control of Metal-Organic Framework Crystallization Investigated by Time-Resolved In Situ X-Ray Scattering. *Angewandte Chemie-International Edition* **50**, 9624-9628, doi:10.1002/anie.201101757 (2011).
- 70 Saha, S. *et al.* Insight into Fast Nucleation and Growth of Zeolitic Imidazolate Framework-71 by In Situ Time-Resolved Light and X-ray Scattering Experiments. *Crystal Growth & Design* **16**, 2002-2010, doi:10.1021/acs.cgd.5b01594 (2016).
- 71 Chen, D., Zhao, J., Zhang, P. & Dai, S. Mechanochemical synthesis of metal-organic frameworks. *Polyhedron* **162**, 59-64, doi:<https://doi.org/10.1016/j.poly.2019.01.024> (2019).
- 72 Stolar, T. & Užarević, K. Mechanochemistry: an efficient and versatile toolbox for synthesis, transformation, and functionalization of porous metal-organic frameworks. *CrystEngComm* **22**, 4511-4525, doi:10.1039/D0CE00091D (2020).
- 73 Julien, P. A. *et al.* In Situ Monitoring and Mechanism of the Mechanochemical Formation of a Microporous MOF-74 Framework. *Journal of the American Chemical Society* **138**, 2929-2932, doi:10.1021/jacs.5b13038 (2016).

- 74 Katsenis, A. D. *et al.* In situ X-ray diffraction monitoring of a mechanochemical reaction reveals a unique topology metal-organic framework. *Nature Communications* **6**, 6662, doi:10.1038/ncomms7662 (2015).
- 75 Boldon, L., Laliberte, F. & Liu, L. Review of the fundamental theories behind small angle X-ray scattering, molecular dynamics simulations, and relevant integrated application. *Nano Reviews* **6**, 25661, doi:10.3402/nano.v6.25661 (2015).
- 76 Holder, C. F. & Schaak, R. E. Tutorial on Powder X-ray Diffraction for Characterizing Nanoscale Materials. *ACS Nano* **13**, 7359-7365, doi:10.1021/acsnano.9b05157 (2019).
- 77 Holton, J. M. & Frankel, K. A. The minimum crystal size needed for a complete diffraction data set. *Acta Crystallographica Section D* **66**, 393-408, doi:doi:10.1107/S0907444910007262 (2010).
- 78 Joy, D. C. THE THEORY AND PRACTICE OF HIGH-RESOLUTION SCANNING ELECTRON-MICROSCOPY. *Ultramicroscopy* **37**, 216-233, doi:10.1016/0304-3991(91)90020-7 (1991).
- 79 Gross, L., Mohn, F., Moll, N., Liljeroth, P. & Meyer, G. The Chemical Structure of a Molecule Resolved by Atomic Force Microscopy. *Science* **325**, 1110-1114, doi:10.1126/science.1176210 (2009).
- 80 Xing, J. F., Schweighauser, L., Okada, S., Harano, K. & Nakamura, E. Atomistic structures and dynamics of prenucleation clusters in MOF-2 and MOF-5 syntheses. *Nature Communications* **10**, doi:10.1038/s41467-019-11564-4 (2019).
- 81 Hermes, S. *et al.* Trapping metal-organic framework nanocrystals: An in-situ time-resolved light scattering study on the crystal growth of MOF-5 in solution. *Journal of the American Chemical Society* **129**, 5324+, doi:10.1021/ja068835i (2007).
- 82 Moh, P. Y., Cubillas, P., Anderson, M. W. & Attfield, M. P. Revelation of the Molecular Assembly of the Nanoporous Metal Organic Framework ZIF-8. *Journal of the American Chemical Society* **133**, 13304-13307, doi:10.1021/ja205900f (2011).
- 83 Mandemaker, L. D. B. *et al.* Time-Resolved In Situ Liquid-Phase Atomic Force Microscopy and Infrared Nanospectroscopy during the Formation of Metal-Organic Framework Thin Films. *Journal of Physical Chemistry Letters* **9**, 1838-1844, doi:10.1021/acs.jpcllett.8b00203 (2018).
- 84 Falke, S. & Betzel, C. in *Radiation in Bioanalysis: Spectroscopic Techniques and Theoretical Methods* (eds Alice S. Pereira, Pedro Tavares, & Paulo Limão-Vieira) 173-193 (Springer International Publishing, 2019).
- 85 van der Veen, M. A., Verbiest, T. & De Vos, D. E. Probing microporous materials with second-harmonic generation. *Microporous and Mesoporous Materials* **166**, 102-108, doi:10.1016/j.micromeso.2012.04.051 (2013).
- 86 Van Cleuvenbergen, S. *et al.* Morphology and structure of ZIF-8 during crystallisation measured by dynamic angle-resolved second harmonic scattering. *Nature Communications* **9**, doi:10.1038/s41467-018-05713-4 (2018).
- 87 Nikitenko, S. *et al.* Implementation of a combined SAXS/WAXS/QEXAFS set-up for time-resolved in situ experiments. *Journal of Synchrotron Radiation* **15**, 632-640, doi:10.1107/s0909049508023327 (2008).
- 88 Goesten, M. *et al.* The Molecular Pathway to ZIF-7 Microrods Revealed by In Situ Time-Resolved Small- and Wide-Angle X-Ray Scattering, Quick-Scanning Extended X-Ray Absorption Spectroscopy, and DFT Calculations. *Chemistry-a European Journal* **19**, 7809-7816, doi:10.1002/chem.201204638 (2013).
- 89 Hughes, C. E., Williams, P. A. & Harris, K. D. M. "CLASSIC NMR": An In-Situ NMR Strategy for Mapping the Time-Evolution of Crystallization Processes by Combined Liquid-State and Solid-State Measurements. *Angewandte Chemie-International Edition* **53**, 8939-8943, doi:10.1002/anie.201404266 (2014).
- 90 Jones, C. L. *et al.* Exploiting in situ NMR to monitor the formation of a metal-organic framework. *Chemical Science* **12**, 1486-1494, doi:10.1039/d0sc04892e (2021).
- 91 Zhao, J. J., Kalanyan, B., Barton, H. F., Sperling, B. A. & Parsons, G. N. In Situ Time-Resolved Attenuated Total Reflectance Infrared Spectroscopy for Probing Metal-Organic Framework

- Thin Film Growth. *Chemistry of Materials* **29**, 8804-8810, doi:10.1021/acs.chemmater.7b03096 (2017).
- 92 Embrechts, H. *et al.* Elucidation of the Formation Mechanism of Metal-Organic Frameworks via in-Situ Raman and FTIR Spectroscopy under Solvothermal Conditions. *Journal of Physical Chemistry C* **122**, 12267-12278, doi:10.1021/acs.jpcc.8b02484 (2018).
- 93 Embrechts, H. *et al.* In situ Raman and FTIR spectroscopic study on the formation of the isomers MIL-68(Al) and MIL-53(Al). *Rsc Advances* **10**, 7336-7348, doi:10.1039/c9ra09968a (2020).
- 94 Li, H. *et al.* Recent advances in gas storage and separation using metal-organic frameworks. *Materials Today* **21**, 108-121, doi:10.1016/j.mattod.2017.07.006 (2018).
- 95 Cai, W. *et al.* Metal Organic Framework-Based Stimuli-Responsive Systems for Drug Delivery. *Advanced Science* **6**, doi:10.1002/advs.201801526 (2019).
- 96 Xie, L. S., Skorupskii, G. & Dinca, M. Electrically Conductive Metal-Organic Frameworks. *Chemical Reviews* **120**, 8536-8580, doi:10.1021/acs.chemrev.9b00766 (2020).
- 97 Escorihuela, J., Narducci, R., Compan, V. & Costantino, F. Proton Conductivity of Composite Polyelectrolyte Membranes with Metal-Organic Frameworks for Fuel Cell Applications. *Advanced Materials Interfaces* **6**, doi:10.1002/admi.201801146 (2019).
- 98 Johnson, C. S. Diffusion ordered nuclear magnetic resonance spectroscopy: principles and applications. *Progress in Nuclear Magnetic Resonance Spectroscopy* **34**, 203-256, doi:10.1016/s0079-6565(99)00003-5 (1999).
- 99 Stallmach, F. & Karger, J. The potentials of pulsed field gradient NMR for investigation of porous media. *Adsorption-Journal of the International Adsorption Society* **5**, 117-133, doi:10.1023/a:1008949607093 (1999).
- 100 Price, W. S. Pulsed-field gradient nuclear magnetic resonance as a tool for studying translational diffusion .1. Basic theory. *Concepts in Magnetic Resonance* **9**, 299-336, doi:10.1002/(sici)1099-0534(1997)9:5<299::Aid-cmr2>3.0.Co;2-u (1997).
- 101 Chmelik, C., Freude, D., Bux, H. & Haase, J. Ethene/ethane mixture diffusion in the MOF sieve ZIF-8 studied by MAS PFG NMR diffusometry. *Microporous and Mesoporous Materials* **147**, 135-141, doi:10.1016/j.micromeso.2011.06.009 (2012).
- 102 Kundu, A., Sillar, K. & Sauer, J. Predicting adsorption selectivities from pure gas isotherms for gas mixtures in metal-organic frameworks. *Chemical Science* **11**, 643-655, doi:10.1039/C9SC03008E (2020).
- 103 Freude, D. *et al.* NMR Study of the Host Structure and Guest Dynamics Investigated with Alkane/Alkene Mixtures in Metal Organic Frameworks ZIF-8. *Journal of Physical Chemistry C* **123**, 1904-1912, doi:10.1021/acs.jpcc.8b11673 (2019).
- 104 Dvoyashkina, N. *et al.* Alkane/alkene mixture diffusion in silicalite-1 studied by MAS PFG NMR. *Microporous and Mesoporous Materials* **257**, 128-134, doi:10.1016/j.micromeso.2017.08.015 (2018).
- 105 Forman, E. M. *et al.* Ethylene diffusion in crystals of zeolitic imidazole Framework-11 embedded in polymers to form mixed-matrix membranes. *Microporous and Mesoporous Materials* **274**, 163-170, doi:10.1016/j.micromeso.2018.07.044 (2019).
- 106 Forse, A. C. *et al.* Unexpected Diffusion Anisotropy of Carbon Dioxide in the Metal-Organic Framework Zn-2(dobpdc). *Journal of the American Chemical Society* **140**, 1663-1673, doi:10.1021/jacs.7b09453 (2018).
- 107 Popp, T. M. O., Plantz, A. Z., Yaghi, O. M. & Reimer, J. A. Precise Control of Molecular Self-Diffusion in Isorecticular and Multivariate Metal-Organic Frameworks. *Chemphyschem* **21**, 32-35, doi:10.1002/cphc.201901043 (2020).
- 108 Walenzus, F., Bon, V., Evans, J. D., Kaskel, S. & Dvoyashkin, M. Molecular Diffusion in a Flexible Mesoporous Metal-Organic Framework over the Course of Structural Contraction. *The Journal of Physical Chemistry Letters* **11**, 9696-9701, doi:10.1021/acs.jpcllett.0c02745 (2020).
- 109 Tan, K. & Chabal, Y. J. in *Metal-Organic Frameworks* (eds Fahmina Zafar & Eram Sharmin) (IntechOpen, 2016).

- 110 Drenchev, N. L. *et al.* In situ FTIR Spectroscopy as a Tool for Investigation of Gas/Solid Interaction: Water-Enhanced CO₂ Adsorption in UiO-66 Metal-Organic Framework. *Journal of Visualized Experiments*, doi:10.3791/60285 (2020).
- 111 Musto, P., Ragosta, G. & Mensitieri, G. Time-resolved FTIR/FTNIR spectroscopy: powerful tools to investigate diffusion processes in polymeric films and membranes. *e-Polymers* **2**, doi:doi:10.1515/epoly.2002.2.1.220 (2002).
- 112 Karge, H. G. Infrared spectroscopic investigation of diffusion, co-diffusion and counter-diffusion of hydrocarbon molecules in zeolites. *Comptes Rendus Chimie* **8**, 303-319, doi:10.1016/j.crci.2005.01.008 (2005).
- 113 Karimi, M., Tashvigh, A. A., Asadi, F. & Ashtiani, F. Z. Determination of concentration-dependent diffusion coefficient of seven solvents in polystyrene systems using FTIR-ATR technique: experimental and mathematical studies. *Rsc Advances* **6**, 9013-9022, doi:10.1039/c5ra25244j (2016).
- 114 Sharp, C. H. *et al.* Alkane-OH Hydrogen Bond Formation and Diffusion Energetics of n-Butane within UiO-66. *Journal of Physical Chemistry C* **121**, 8902-8906, doi:10.1021/acs.jpcc.7b01351 (2017).
- 115 Grissom, T. G. *et al.* Benzene, Toluene, and Xylene Transport through UiO-66: Diffusion Rates, Energetics, and the Role of Hydrogen Bonding. *Journal of Physical Chemistry C* **122**, 16060-16069, doi:10.1021/acs.jpcc.8b03356 (2018).
- 116 Embs, J. P., Juranyi, F. & Hempelmann, R. Introduction to Quasielastic Neutron Scattering. *Zeitschrift Fur Physikalische Chemie-International Journal of Research in Physical Chemistry & Chemical Physics* **224**, 5-32, doi:10.1524/zpch.2010.6090 (2010).
- 117 Bee, M. Localized and long-range diffusion in condensed matter: state of the art of QENS studies and future prospects. *Chemical Physics* **292**, 121-141, doi:10.1016/s0301-0104(03)00257-x (2003).
- 118 Kolokolov, D. I. *et al.* Diffusion of Benzene in the Breathing Metal-Organic Framework MIL-53(Cr): A Joint Experimental-Computational Investigation. *Journal of Physical Chemistry C* **119**, 8217-8225, doi:10.1021/acs.jpcc.5b01465 (2015).
- 119 Rosenbach, N. *et al.* Quasi-elastic neutron scattering and molecular dynamics study of methane diffusion in metal organic frameworks MIL-47(V) and MIL-53(Cr). *Angewandte Chemie-International Edition* **47**, 6611-6615, doi:10.1002/anie.200801748 (2008).
- 120 Yang, Q. Y. *et al.* Understanding the Thermodynamic and Kinetic Behavior of the CO₂/CH₄ Gas Mixture within the Porous Zirconium Terephthalate UiO-66(Zr): A Joint Experimental and Modeling Approach. *Journal of Physical Chemistry C* **115**, 13768-13774, doi:10.1021/jp202633t (2011).
- 121 Krishna, R. & van Baten, J. M. Insights into diffusion of gases in zeolites gained from molecular dynamics simulations. *Microporous and Mesoporous Materials* **109**, 91-108, doi:10.1016/j.micromeso.2007.04.036 (2008).
- 122 Forman, E. M., Pimentel, B. R., Ziegler, K. J., Lively, R. P. & Vasenkov, S. Microscopic diffusion of pure and mixed methane and carbon dioxide in ZIF-11 by high field diffusion NMR. *Microporous and Mesoporous Materials* **248**, 158-163, doi:10.1016/j.micromeso.2017.04.041 (2017).
- 123 Ghoufi, A. & Maurin, G. Single-File Diffusion of Neo-Pentane Confined in the MIL-47(V) Metal-Organic Framework. *Journal of Physical Chemistry C* **123**, 17360-17367, doi:10.1021/acs.jpcc.9b04308 (2019).
- 124 Kärger, J., Heinke, L., Kortunov, P. & Vasenkov, S. in *Studies in Surface Science and Catalysis* Vol. 170 (eds Ruren Xu, Zi Gao, Jiesheng Chen, & Wenfu Yan) 739-747 (Elsevier, 2007).
- 125 Schemmert, U., Karger, J. & Weitkamp, J. Interference microscopy as a technique for directly measuring intracrystalline transport diffusion in zeolites. *Microporous and Mesoporous Materials* **32**, 101-110, doi:10.1016/s1387-1811(99)00095-5 (1999).
- 126 Heinke, L., Kortunov, P., Tzoulaki, D. & Karger, J. The options of interference microscopy to explore the significance of intracrystalline diffusion and surface permeation for overall mass

- transfer on nanoporous materials. *Adsorption-Journal of the International Adsorption Society* **13**, 215-223, doi:10.1007/s10450-007-9048-y (2007).
- 127 Karger, J. & Ruthven, D. M. Diffusion in nanoporous materials: fundamental principles, insights and challenges. *New Journal of Chemistry* **40**, 4027-4048, doi:10.1039/c5nj02836a (2016).
- 128 Chmelik, C., Glaser, R., Haase, J., Hwang, S. & Karger, J. Application of microimaging to diffusion studies in nanoporous materials. *Adsorption-Journal of the International Adsorption Society*, doi:10.1007/s10450-020-00279-4 (2020).
- 129 Heinke, L. *et al.* Three-dimensional diffusion in nanoporous host-guest materials monitored by interference microscopy. *Epl* **81**, doi:10.1209/0295-5075/81/26002 (2008).
- 130 Kortunov, P. V. *et al.* Intracrystalline diffusivities and surface permeabilities deduced from transient concentration profiles: Methanol in MOF manganese formate. *Journal of the American Chemical Society* **129**, 8041-8047, doi:10.1021/ja071265h (2007).
- 131 Briggs, L. *et al.* Binding and separation of CO₂, SO₂ and C₂H₂ in homo- and hetero-metallic metal-organic framework materials. *Journal of Materials Chemistry A* **9**, 7190-7197, doi:10.1039/D1TA00687H (2021).
- 132 Krap, C. P. *et al.* Enhancement of CO₂ Adsorption and Catalytic Properties by Fe-Doping of [Ga₂(OH)₂(L)] (H₄L = Biphenyl-3,3',5,5'-tetracarboxylic Acid), MFM-300(Ga₂). **55**, 1076-1088, doi:10.1021/acs.inorgchem.5b02108 (2016).
- 133 Savage, M. *et al.* Selective Adsorption of Sulfur Dioxide in a Robust Metal-Organic Framework Material. *Advanced Materials* **28**, 8705-8711, doi:<https://doi.org/10.1002/adma.201602338> (2016).
- 134 Smith, G. L. *et al.* Reversible coordinative binding and separation of sulfur dioxide in a robust metal-organic framework with open copper sites. *Nature Materials* **18**, 1358-1365, doi:10.1038/s41563-019-0495-0 (2019).
- 135 Greenaway, A. *et al.* In situ Synchrotron IR Microspectroscopy of CO₂ Adsorption on Single Crystals of the Functionalized MOF Sc-2(BDC-NH₂)(3). *Angewandte Chemie-International Edition* **53**, 13483-13487, doi:10.1002/anie.201408369 (2014).
- 136 Godfrey, H. G. W. *et al.* Ammonia Storage by Reversible Host-Guest Site Exchange in a Robust Metal-Organic Framework. *Angewandte Chemie International Edition* **57**, 14778-14781, doi:<https://doi.org/10.1002/anie.201808316> (2018).
- 137 Humby, J. D. *et al.* Host-guest selectivity in a series of isorecticular metal-organic frameworks: observation of acetylene-to-alkyne and carbon dioxide-to-amide interactions. *Chemical Science* **10**, 1098-1106, doi:10.1039/C8SC03622E (2019).
- 138 Souza, B. E. *et al.* Elucidating the Drug Release from Metal-Organic Framework Nanocomposites via In Situ Synchrotron Microspectroscopy and Theoretical Modeling. *Acs Applied Materials & Interfaces* **12**, 5147-5156, doi:10.1021/acsami.9b21321 (2020).
- 139 Bux, H., Chmelik, C., Krishna, R. & Caro, J. Ethene/ethane separation by the MOF membrane ZIF-8: Molecular correlation of permeation, adsorption, diffusion. *Journal of Membrane Science* **369**, 284-289, doi:10.1016/j.memsci.2010.12.001 (2011).
- 140 Baniani, A. *et al.* Anomalous Relationship between Molecular Size and Diffusivity of Ethane and Ethylene inside Crystals of Zeolitic Imidazolate Framework-11. *Journal of Physical Chemistry C* **123**, 16813-16822, doi:10.1021/acs.jpcc.9b03933 (2019).
- 141 Berens, S. *et al.* Ethane diffusion in mixed linker zeolitic imidazolate framework-7-8 by pulsed field gradient NMR in combination with single crystal IR microscopy. *Physical Chemistry Chemical Physics* **20**, 23967-23975, doi:10.1039/c8cp04889d (2018).
- 142 Czanderna, A. W. & Lu, C. in *Methods and Phenomena* Vol. 7 (eds C. Lu & A. W. Czanderna) 1-18 (Elsevier, 1984).
- 143 Kanazawa, K. & Cho, N.-J. Quartz Crystal Microbalance as a Sensor to Characterize Macromolecular Assembly Dynamics. *Journal of Sensors* **2009**, 824947, doi:10.1155/2009/824947 (2009).

- 144 Tuantranont, A., Wisitsora-at, A., Sritongkham, P. & Jaruwongrungrsee, K. A review of monolithic multichannel quartz crystal microbalance: A review. *Analytica Chimica Acta* **687**, 114-128, doi:10.1016/j.aca.2010.12.022 (2011).
- 145 O'Sullivan, C. K. & Guilbault, G. G. Commercial quartz crystal microbalances - theory and applications. *Biosensors & Bioelectronics* **14**, 663-670, doi:10.1016/s0956-5663(99)00040-8 (1999).
- 146 Wang, L. Y. Metal-organic frameworks for QCM-based gas sensors: A review. *Sensors and Actuators a-Physical* **307**, doi:10.1016/j.sna.2020.111984 (2020).
- 147 Zybaylo, O. *et al.* A novel method to measure diffusion coefficients in porous metal-organic frameworks. *Physical Chemistry Chemical Physics* **12**, 8092-8097, doi:10.1039/b927601g (2010).
- 148 Heinke, L., Gu, Z. G. & Woll, C. The surface barrier phenomenon at the loading of metal-organic frameworks. *Nature Communications* **5**, doi:10.1038/ncomms5562 (2014).
- 149 Zhou, W. C., Woell, C. & Heinke, L. Liquid- and Gas-Phase Diffusion of Ferrocene in Thin Films of Metal-Organic Frameworks. *Materials* **8**, 3767-3775, doi:10.3390/ma8063767 (2015).
- 150 Heinke, L. & Woll, C. Adsorption and diffusion in thin films of nanoporous metal-organic frameworks: ferrocene in SURMOF Cu-2(ndc)(2)(dabco). *Physical Chemistry Chemical Physics* **15**, 9295-9299, doi:10.1039/c3cp50578b (2013).
- 151 Muller, K., Vankova, N., Schottner, L., Heine, T. & Heinke, L. Dissolving uptake-hindering surface defects in metal-organic frameworks. *Chemical Science* **10**, 153-160, doi:10.1039/c8sc03735c (2019).
- 152 Ramaswamy, P., Wong, N. E. & Shimizu, G. K. H. MOFs as proton conductors - challenges and opportunities. *Chemical Society Reviews* **43**, 5913-5932, doi:10.1039/c4cs00093e (2014).
- 153 Lim, D. W. & Kitagawa, H. Proton Transport in Metal-Organic Frameworks. *Chemical Reviews* **120**, 8416-8467, doi:10.1021/acs.chemrev.9b00842 (2020).
- 154 Sadakiyo, M., Yamada, T. & Kitagawa, H. Rational Designs for Highly Proton-Conductive Metal-Organic Frameworks. *Journal of the American Chemical Society* **131**, 9906-+, doi:10.1021/ja9040016 (2009).
- 155 Macdonald, J. R. IMPEDANCE SPECTROSCOPY. *Annals of Biomedical Engineering* **20**, 289-305, doi:10.1007/bf02368532 (1992).
- 156 Lee, Y. J., Murakhtina, T., Sebastiani, D. & Spiess, H. W. H-2 solid-state NMR of mobile protons: It is not always the simple way. *Journal of the American Chemical Society* **129**, 12406-+, doi:10.1021/ja0754857 (2007).
- 157 Vilčiauskas, L., Tuckerman, M. E., Bester, G., Paddison, S. J. & Kreuer, K. D. The mechanism of proton conduction in phosphoric acid. *Nature Chemistry* **4**, 461-466, doi:10.1038/nchem.1329 (2012).
- 158 Agmon, N. THE GROTTTHUSS MECHANISM. *Chemical Physics Letters* **244**, 456-462, doi:10.1016/0009-2614(95)00905-j (1995).
- 159 Kreuer, K. D., Rabenau, A. & Weppner, W. VEHICLE MECHANISM, A NEW MODEL FOR THE INTERPRETATION OF THE CONDUCTIVITY OF FAST PROTON CONDUCTORS. *Angewandte Chemie-International Edition in English* **21**, 208-209, doi:10.1002/anie.198202082 (1982).
- 160 Pili, S. *et al.* Proton Conduction in a Phosphonate-Based Metal-Organic Framework Mediated by Intrinsic "Free Diffusion inside a Sphere". *Journal of the American Chemical Society* **138**, 6352-6355, doi:10.1021/jacs.6b02194 (2016).
- 161 Rought, P. *et al.* Modulating proton diffusion and conductivity in metal-organic frameworks by incorporation of accessible free carboxylic acid groups. *Chemical Science* **10**, 1492-1499, doi:10.1039/c8sc03022g (2019).
- 162 Liu, Q. Y. *et al.* Metal Organic Frameworks Modified Proton Exchange Membranes for Fuel Cells. *Frontiers in Chemistry* **8**, doi:10.3389/fchem.2020.00694 (2020).
- 163 Kang, D. W., Kang, M. & Hong, C. S. Post-synthetic modification of porous materials: superprotonic conductivities and membrane applications in fuel cells. *Journal of Materials Chemistry A* **8**, 7474-7494, doi:10.1039/d0ta01733g (2020).

- 164 Liang, X. *et al.* Potential Applications of Metal Organic Framework-Based Materials for Proton Exchange Membrane Fuel Cells. *Progress in Chemistry* **30**, 1770-1783, doi:10.7536/pc171239 (2018).
- 165 Baumann, A. E., Burns, D. A., Liu, B. Q. & Thoi, V. S. Metal-organic framework functionalization and design strategies for advanced electrochemical energy storage devices. *Communications Chemistry* **2**, doi:10.1038/s42004-019-0184-6 (2019).
- 166 Choi, K. M. *et al.* Supercapacitors of Nanocrystalline Metal-Organic Frameworks. *ACS Nano* **8**, 7451-7457, doi:10.1021/nn5027092 (2014).
- 167 Liang, H. Q. *et al.* A Light-Responsive Metal-Organic Framework Hybrid Membrane with High On/Off Photoswitchable Proton Conductivity. *Angewandte Chemie-International Edition* **59**, 7732-7737, doi:10.1002/anie.202002389 (2020).
- 168 Kanj, A. B. *et al.* Proton-conduction photomodulation in spiropyran-functionalized MOFs with large on-off ratio. *Chemical Science* **11**, 1404-1410, doi:10.1039/c9sc04926f (2020).
- 169 Liang, H. Q., Guo, Y., Peng, X. S. & Chen, B. L. Light-gated cation-selective transport in metal-organic framework membranes. *Journal of Materials Chemistry A* **8**, 11399-11405, doi:10.1039/d0ta02895a (2020).
- 170 Muller, K. *et al.* Switching the Proton Conduction in Nanoporous, Crystalline Materials by Light. *Advanced Materials* **30**, doi:10.1002/adma.201706551 (2018).
- 171 Song, Y. *et al.* Transformation of a proton insulator to a conductor via reversible amorphous to crystalline structure transformation of MOFs. *Chemical Communications* **56**, 4468-4471, doi:10.1039/d0cc00755b (2020).
- 172 Wei, Y. S. *et al.* Unique Proton Dynamics in an Efficient MOF-Based Proton Conductor. *Journal of the American Chemical Society* **139**, 3505-3512, doi:10.1021/jacs.6b12847 (2017).
- 173 Shen, L. *et al.* Creating Lithium-Ion Electrolytes with Biomimetic Ionic Channels in Metal-Organic Frameworks. *Advanced Materials* **30**, 1707476, doi:<https://doi.org/10.1002/adma.201707476> (2018).
- 174 Fujie, K., Yamada, T., Ikeda, R. & Kitagawa, H. Introduction of an Ionic Liquid into the Micropores of a Metal-Organic Framework and Its Anomalous Phase Behavior. *Angewandte Chemie International Edition* **53**, 11302-11305, doi:<https://doi.org/10.1002/anie.201406011> (2014).
- 175 Kinik, F. P., Uzun, A. & Keskin, S. Ionic Liquid/Metal-Organic Framework Composites: From Synthesis to Applications. *ChemSusChem* **10**, 2842-2863, doi:<https://doi.org/10.1002/cssc.201700716> (2017).
- 176 Kanj, A. B. *et al.* Bunching and Immobilization of Ionic Liquids in Nanoporous Metal-Organic Framework. *Nano Letters* **19**, 2114-2120, doi:10.1021/acs.nanolett.8b04694 (2019).
- 177 Wang, H. F., Chen, L. Y., Pang, H., Kaskel, S. & Xu, Q. MOF-derived electrocatalysts for oxygen reduction, oxygen evolution and hydrogen evolution reactions. *Chemical Society Reviews* **49**, 1414-1448, doi:10.1039/c9cs00906j (2020).
- 178 Cheng, W. R. *et al.* Lattice-strained metal-organic-framework arrays for bifunctional oxygen electrocatalysis (vol 4, pg 115, 2019). *Nature Energy* **5**, 346-347, doi:10.1038/s41560-020-0599-4 (2020).
- 179 Yan, Z. H. *et al.* Photo-generated dinuclear {Eu(II)}₂ active sites for selective CO₂ reduction in a photosensitizing metal-organic framework. *Nature Communications* **9**, doi:10.1038/s41467-018-05659-7 (2018).
- 180 Xia, B. Y. *et al.* A metal-organic framework-derived bifunctional oxygen electrocatalyst. *Nature Energy* **1**, doi:10.1038/nenergy.2015.6 (2016).
- 181 Zhao, Y. *et al.* Metal organic frameworks for energy storage and conversion. *Energy Storage Materials* **2**, 35-62, doi:10.1016/j.ensm.2015.11.005 (2016).
- 182 Wang, L. *et al.* Metal-organic frameworks for energy storage: Batteries and supercapacitors. *Coordination Chemistry Reviews* **307**, 361-381, doi:10.1016/j.ccr.2015.09.002 (2016).
- 183 Feng, D. W. *et al.* Robust and conductive two-dimensional metal-organic frameworks with exceptionally high volumetric and areal capacitance. *Nature Energy* **3**, 30-36, doi:10.1038/s41560-017-0044-5 (2018).

- 184 Sheberla, D. *et al.* Conductive MOF electrodes for stable supercapacitors with high areal capacitance. *Nature Materials* **16**, 220-224, doi:10.1038/nmat4766 (2017).
- 185 Deng, R., Han, W. & Yeung, K. L. Confined PFSA/MOF composite membranes in fuel cells for promoted water management and performance. *Catalysis Today* **331**, 12-17, doi:10.1016/j.cattod.2018.05.016 (2019).
- 186 Cai, K. *et al.* An acid-stable hexaphosphate ester based metal-organic framework and its polymer composite as proton exchange membrane. *Journal of Materials Chemistry A* **5**, 12943-12950, doi:10.1039/c7ta00169j (2017).
- 187 Anahidzade, N., Abdolmaleki, A., Dinari, M., Tadavani, K. F. & Zhiani, M. Metal-organic framework anchored sulfonated poly(ether sulfone) as a high temperature proton exchange membrane for fuel cells. *Journal of Membrane Science* **565**, 281-292, doi:10.1016/j.memsci.2018.08.037 (2018).
- 188 Murase, R., Ding, B. W., Gu, Q. Y. & D'Alessandro, D. M. Prospects for electroactive and conducting framework materials. *Philosophical Transactions of the Royal Society a-Mathematical Physical and Engineering Sciences* **377**, doi:10.1098/rsta.2018.0226 (2019).
- 189 Chueh, C. C. *et al.* Harnessing MOF materials in photovoltaic devices: recent advances, challenges, and perspectives. *Journal of Materials Chemistry A* **7**, 17079-17095, doi:10.1039/c9ta03595h (2019).
- 190 Heidary, N., Harris, T., Ly, K. H. & Kornienko, N. Artificial photosynthesis with metal and covalent organic frameworks (MOFs and COFs): challenges and prospects in fuel-forming electrocatalysis. *Physiologia Plantarum* **166**, 460-471, doi:10.1111/ppl.12935 (2019).
- 191 Khitrova, G., Berman, P. R. & Sargent, M. THEORY OF PUMP PROBE SPECTROSCOPY. *Journal of the Optical Society of America B-Optical Physics* **5**, 160-170, doi:10.1364/josab.5.000160 (1988).
- 192 Lytle, F. E., Parrish, R. M. & Barnes, W. T. An Introduction to Time-Resolved Pump/Probe Spectroscopy. *Appl. Spectrosc.* **39**, 444-451 (1985).
- 193 Tromp, M. *et al.* Energy Dispersive XAFS: Characterization of Electronically Excited States of Copper(I) Complexes. *Journal of Physical Chemistry B* **117**, 7381-7387, doi:10.1021/jp4020355 (2013).
- 194 Easun, T. L. *et al.* Photochemistry in a 3D Metal-Organic Framework (MOF): Monitoring Intermediates and Reactivity of the fac-to-mer Photoisomerization of Re(diimine)(CO)(3)Cl Incorporated in a MOF. *Inorganic Chemistry* **53**, 2606-2612, doi:10.1021/ic402955e (2014).
- 195 Blake, A. J. *et al.* Photoreactivity examined through incorporation in metal-organic frameworks. *Nature Chemistry* **2**, 688-694, doi:10.1038/nchem.681 (2010).
- 196 Easun, T. L. *et al.* Modification of coordination networks through a photoinduced charge transfer process. *Chemical Science* **5**, 539-544, doi:10.1039/c3sc52745j (2014).
- 197 Pattengale, B. *et al.* Exceptionally Long-Lived Charge Separated State in Zeolitic Imidazolate Framework: Implication for Photocatalytic Applications. *Journal of the American Chemical Society* **138**, 8072-8075, doi:10.1021/jacs.6b04615 (2016).
- 198 Pattengale, B. *et al.* Metal-Organic Framework Photoconductivity via Time-Resolved Terahertz Spectroscopy. *Journal of the American Chemical Society* **141**, 9793-9797, doi:10.1021/jacs.9b04338 (2019).
- 199 Hanna, L., Kucheryavy, P., Liu, C. M., Zhang, X. Y. & Lockard, J. V. Long-Lived Photoinduced Charge Separation in a Trinuclear Iron- $\mu(3)$ -oxo-based Metal-Organic Framework. *Journal of Physical Chemistry C* **121**, 13570-13576, doi:10.1021/acs.jpcc.7b03936 (2017).
- 200 Yu, J. R., Park, J., Van Wyk, A., Rumbles, G. & Deria, P. Excited-State Electronic Properties in Zr-Based Metal-Organic Frameworks as a Function of a Topological Network. *Journal of the American Chemical Society* **140**, 10488-10496, doi:10.1021/jacs.8b04980 (2018).
- 201 Li, X. X. *et al.* Ultrafast Relaxation Dynamics in Zinc Tetraphenylporphyrin Surface-Mounted Metal Organic Framework. *Journal of Physical Chemistry C* **122**, 50-61, doi:10.1021/acs.jpcc.7b08696 (2018).
- 202 Rodriguez, A. M. B. *et al.* Ligand-to-diimine/metal-to-diimine charge-transfer excited states of Re(NCS)(CO)(3)(α -diimine) (α -diimine=2,2'-bipyridine, di-Pr-i-N,N-1,4-

- diazabutadiene). A spectroscopic and computational study. *Journal of Physical Chemistry A* **109**, 5016-5025, doi:10.1021/jp044114z (2005).
- 203 Mitra, T. *et al.* Characterisation of redox states of metal–organic frameworks by growth on modified thin-film electrodes. *Chemical Science* **9**, 6572-6579, doi:10.1039/C8SC00803E (2018).
- 204 Hua, C. *et al.* Through-Space Intervalence Charge Transfer as a Mechanism for Charge Delocalization in Metal-Organic Frameworks. *Journal of the American Chemical Society* **140**, 6622-6630, doi:10.1021/jacs.8b02638 (2018).
- 205 Ding, B. W., Hua, C., Kepert, C. J. & D'Alessandro, D. M. Influence of structure-activity relationships on through-space intervalence charge transfer in metal-organic frameworks with cofacial redox-active units. *Chemical Science* **10**, 1392-1400, doi:10.1039/c8sc01128a (2019).
- 206 Usov, P. M. *et al.* Probing charge transfer characteristics in a donor-acceptor metal-organic framework by Raman spectroelectrochemistry and pressure-dependence studies. *Physical Chemistry Chemical Physics* **20**, 25772-25779, doi:10.1039/c8cp04157a (2018).
- 207 Garg, S. *et al.* Conductance Photoswitching of Metal–Organic Frameworks with Embedded Spiropyran. *Angewandte Chemie International Edition* **58**, 1193-1197, doi:<https://doi.org/10.1002/anie.201811458> (2019).
- 208 Yu, F. *et al.* Photostimulus-Responsive Large-Area Two-Dimensional Covalent Organic Framework Films. *Angewandte Chemie International Edition* **58**, 16101-16104, doi:<https://doi.org/10.1002/anie.201909613> (2019).
- 209 Sun, L., Park, S. S., Sheberla, D. & Dinca, M. Measuring and Reporting Electrical Conductivity in Metal Organic Frameworks: Cd-2(TTFTB) as a Case Study. *Journal of the American Chemical Society* **138**, 14772-14782, doi:10.1021/jacs.6b09345 (2016).
- 210 Narayan, T. C., Miyakai, T., Seki, S. & Dinca, M. High Charge Mobility in a Tetrathiafulvalene-Based Microporous Metal-Organic Framework. *Journal of the American Chemical Society* **134**, 12932-12935, doi:10.1021/ja3059827 (2012).
- 211 Aubrey, M. L. *et al.* Electron delocalization and charge mobility as a function of reduction in a metal-organic framework. *Nature Materials* **17**, 625-+, doi:10.1038/s41563-018-0098-1 (2018).
- 212 Dong, R. *et al.* High-mobility band-like charge transport in a semiconducting two-dimensional metal-organic framework. *Nature Materials* **17**, 1027-+, doi:10.1038/s41563-018-0189-z (2018).
- 213 Cai, M., Loague, Q. & Morris, A. J. Design Rules for Efficient Charge Transfer in Metal-Organic Framework Films: The Pore Size Effect. *Journal of Physical Chemistry Letters* **11**, 702-709, doi:10.1021/acs.jpcllett.9b03285 (2020).
- 214 Halder, A. & Ghoshal, D. Structure and properties of dynamic metal-organic frameworks: a brief accounts of crystalline-to-crystalline and crystalline-to-amorphous transformations. *Crystengcomm* **20**, 1322-1345, doi:10.1039/c7ce02066j (2018).
- 215 Jiang, J. W. Concluding remarks: Cooperative phenomena in framework materials. *Faraday Discussions* **225**, 442-454, doi:10.1039/d0fd90035d (2021).
- 216 Schneemann, A. *et al.* Flexible metal-organic frameworks. *Chemical Society Reviews* **43**, 6062-6096, doi:10.1039/c4cs00101j (2014).
- 217 Krause, S., Hosono, N. & Kitagawa, S. Chemistry of Soft Porous Crystals: Structural Dynamics and Gas Adsorption Properties. *Angewandte Chemie-International Edition* **59**, 15325-15341, doi:10.1002/anie.202004535 (2020).
- 218 Alhamami, M., Doan, H. & Cheng, C. H. A Review on Breathing Behaviors of Metal-Organic-Frameworks (MOFs) for Gas Adsorption. *Materials* **7**, 3198-3250, doi:10.3390/ma7043198 (2014).
- 219 Hyun, S. M. *et al.* Exploration of Gate-Opening and Breathing Phenomena in a Tailored Flexible Metal-Organic Framework. *Inorganic Chemistry* **55**, 1920-1925, doi:10.1021/acs.inorgchem.5b02874 (2016).

- 220 Chang, Z., Yang, D. H., Xu, J., Hu, T. L. & Bu, X. H. Flexible Metal-Organic Frameworks: Recent
Advances and Potential Applications. *Advanced Materials* **27**, 5432-5441,
doi:10.1002/adma.201501523 (2015).
- 221 Burtch, N. C. *et al.* In situ visualization of loading-dependent water effects in a stable metal-
organic framework. *Nature Chemistry* **12**, 186-192, doi:10.1038/s41557-019-0374-y (2020).
- 222 Lo, S. H. *et al.* Rapid desolvation-triggered domino lattice rearrangement in a metal-organic
framework. *Nature Chemistry* **12**, 90-97, doi:10.1038/s41557-019-0364-0 (2020).
- 223 Krause, S. *et al.* Towards general network architecture design criteria for negative gas
adsorption transitions in ultraporous frameworks. *Nature Communications* **10**,
doi:10.1038/s41467-019-11565-3 (2019).
- 224 Krause, S. *et al.* The effect of crystallite size on pressure amplification in switchable porous
solids. *Nature Communications* **9**, doi:10.1038/s41467-018-03979-2 (2018).
- 225 Carrington, E. J. *et al.* Solvent-switchable continuous-breathing behaviour in a diamondoid
metal-organic framework and its influence on CO₂ versus CH₄ selectivity. *Nature Chemistry*
9, 882-889, doi:10.1038/nchem.2747 (2017).
- 226 Serra-Crespo, P. *et al.* Experimental evidence of negative linear compressibility in the MIL-53
metal-organic framework family. *Crystengcomm* **17**, 276-280, doi:10.1039/c4ce00436a
(2015).
- 227 Li, W. *et al.* Negative Linear Compressibility of a Metal-Organic Framework. *Journal of the
American Chemical Society* **134**, 11940-11943, doi:10.1021/ja305196u (2012).
- 228 Zeng, Q. X., Wang, K., Qiao, Y. C., Li, X. D. & Zou, B. Negative Linear Compressibility Due to
Layer Sliding in a Layered Metal-Organic Framework. *Journal of Physical Chemistry Letters* **8**,
1436-1441, doi:10.1021/acs.jpcclett.7b00121 (2017).
- 229 Cai, W. Z. & Katrusiak, A. Giant negative linear compression positively coupled to massive
thermal expansion in a metal-organic framework. *Nature Communications* **5**,
doi:10.1038/ncomms5337 (2014).
- 230 Yousef, H. *et al.* Timepix3 as X-ray detector for time resolved synchrotron experiments.
*Nuclear Instruments & Methods in Physics Research Section a-Accelerators Spectrometers
Detectors and Associated Equipment* **845**, 639-643, doi:10.1016/j.nima.2016.04.075 (2017).
- 231 Poikela, T. *et al.* Timepix3: a 65K channel hybrid pixel readout chip with simultaneous
ToA/ToT and sparse readout. *Journal of Instrumentation* **9**, doi:10.1088/1748-
0221/9/05/c05013 (2014).
- 232 Castillo-Blas, C., Moreno, J. M., Romero-Muñiz, I. & Platero-Prats, A. E. Applications of pair
distribution function analyses to the emerging field of non-ideal metal-organic framework
materials. *Nanoscale* **12**, 15577-15587, doi:10.1039/D0NR01673J (2020).
- 233 Mao, H. Y., Xu, J., Hu, Y., Huang, Y. N. & Song, Y. The effect of high external pressure on the
structure and stability of MOF alpha-Mg-3(HCOO)₆ probed by in situ Raman and FT-IR
spectroscopy. *Journal of Materials Chemistry A* **3**, 11976-11984, doi:10.1039/c5ta00476d
(2015).
- 234 Ryder, M. R. *et al.* Tracking thermal-induced amorphization of a zeolitic imidazolate
framework via synchrotron in situ far-infrared spectroscopy. *Chemical Communications* **53**,
7041-7044, doi:10.1039/c7cc01985h (2017).
- 235 Nishida, J. *et al.* Structural dynamics inside a functionalized metal-organic framework probed
by ultrafast 2D IR spectroscopy. *Proceedings of the National Academy of Sciences of the
United States of America* **111**, 18442-18447, doi:10.1073/pnas.1422194112 (2014).
- 236 Nishida, J. & Fayer, M. D. Guest Hydrogen Bond Dynamics and Interactions in the Metal-
Organic Framework MIL-53(Al) Measured with Ultrafast Infrared Spectroscopy. *Journal of
Physical Chemistry C* **121**, 11880-11890, doi:10.1021/acs.jpcc.7b02458 (2017).
- 237 Le Sueur, A. L., Horness, R. E. & Thielges, M. C. Applications of two-dimensional infrared
spectroscopy. *Analyst* **140**, 4336-4349, doi:10.1039/c5an00558b (2015).
- 238 Coudert, F.-X. Responsive Metal-Organic Frameworks and Framework Materials: Under
Pressure, Taking the Heat, in the Spotlight, with Friends. *Chemistry of Materials* **27**, 1905-
1916, doi:10.1021/acs.chemmater.5b00046 (2015).

- 239 Castellanos, S., Kapteijn, F. & Gascon, J. Photoswitchable metal organic frameworks: turn on the lights and close the windows. *CrystEngComm* **18**, 4006-4012, doi:10.1039/C5CE02543E (2016).
- 240 Mutruc, D. *et al.* Modulating Guest Uptake in Core-Shell MOFs with Visible Light. *Angewandte Chemie-International Edition* **58**, 12862-12867, doi:10.1002/anie.201906606 (2019).
- 241 Liu, C. Y., Jiang, Y. Z., Zhou, C., Caro, J. & Huang, A. S. Photo-switchable smart metal organic framework membranes with tunable and enhanced molecular sieving performance. *Journal of Materials Chemistry A* **6**, 24949-24955, doi:10.1039/c8ta10541c (2018).
- 242 Wang, Z. *et al.* Tunable molecular separation by nanoporous membranes. *Nature Communications* **7**, 13872, doi:10.1038/ncomms13872 (2016).
- 243 Williams, D. E. *et al.* Flipping the Switch: Fast Photoisomerization in a Confined Environment. *Journal of the American Chemical Society* **140**, 7611-7622, doi:10.1021/jacs.8b02994 (2018).
- 244 Hoffmann, H. C. *et al.* High-Pressure in Situ Xe-129 NMR Spectroscopy and Computer Simulations of Breathing Transitions in the Metal-Organic Framework Ni-2(2,6-ndc)(2)(dabco) (DUT-8(Ni)). *Journal of the American Chemical Society* **133**, 8681-8690, doi:10.1021/ja201951t (2011).
- 245 Schaber, J. *et al.* In Situ Monitoring of Unique Switching Transitions in the Pressure Amplifying Flexible Framework Material DUT-49 by High-Pressure Xe-129 NMR Spectroscopy. *Journal of Physical Chemistry C* **121**, 5195-5200, doi:10.1021/acs.jpcc.7b01204 (2017).
- 246 Kolbe, F. *et al.* High-Pressure in Situ Xe-129 NMR Spectroscopy: Insights into Switching Mechanisms of Flexible Metal-Organic Frameworks Isorecticular to DUT-49. *Chemistry of Materials* **31**, 6193-6201, doi:10.1021/acs.chemmater.9b02003 (2019).
- 247 Bertmer, M. in *Annual Reports on Nmr Spectroscopy, Vol 101* Vol. 101 *Annual Reports on NMR Spectroscopy* (ed AttaurRahman) 1-64 (2020).
- 248 Chen, W., Wu, Y. N. & Li, F. T. Hierarchical Structure and Molecular Dynamics of Metal-Organic Framework as Characterized by Solid State NMR. *Journal of Chemistry* **2016**, doi:10.1155/2016/6510253 (2016).
- 249 Bernin, D. & Hedin, N. Perspectives on NMR studies of CO₂ adsorption. *Current Opinion in Colloid & Interface Science* **33**, 53-62, doi:10.1016/j.cocis.2018.02.003 (2018).
- 250 Moreau, F. *et al.* Tailoring porosity and rotational dynamics in a series of octacarboxylate metal-organic frameworks. *Proceedings of the National Academy of Sciences* **114**, 3056, doi:10.1073/pnas.1615172114 (2017).
- 251 Trenholme, W. J. F. *et al.* Selective Gas Uptake and Rotational Dynamics in a (3,24)-Connected Metal-Organic Framework Material. *Journal of the American Chemical Society* **143**, 3348-3358, doi:10.1021/jacs.0c11202 (2021).
- 252 Sin, M. *et al.* In Situ C-13 NMR Spectroscopy Study of CO₂/CH₄ Mixture Adsorption by Metal-Organic Frameworks: Does Flexibility Influence Selectivity? *Langmuir* **35**, 3162-3170, doi:10.1021/acs.langmuir.8b03554 (2019).
- 253 Benson, O. *et al.* Amides Do Not Always Work: Observation of Guest Binding in an Amide-Functionalized Porous Metal-Organic Framework. *Journal of the American Chemical Society* **138**, 14828-14831, doi:10.1021/jacs.6b08059 (2016).
- 254 Lu, Z. *et al.* Modulating supramolecular binding of carbon dioxide in a redox-active porous metal-organic framework. *Nature Communications* **8**, 14212, doi:10.1038/ncomms14212 (2017).
- 255 Moreau, F. *et al.* Unravelling exceptional acetylene and carbon dioxide adsorption within a tetra-amide functionalized metal-organic framework. *Nature Communications* **8**, 14085, doi:10.1038/ncomms14085 (2017).
- 256 Zhou, W. & Yildirim, T. Lattice dynamics of metal-organic frameworks: Neutron inelastic scattering and first-principles calculations. *Physical Review B* **74**, doi:10.1103/PhysRevB.74.180301 (2006).

- 257 Zhao, P. *et al.* Structural dynamics of a metal-organic framework induced by CO₂ migration in its non-uniform porous structure. *Nature Communications* **10**, doi:10.1038/s41467-019-08939-y (2019).
- 258 Auckett, J. E. *et al.* Continuous negative-to-positive tuning of thermal expansion achieved by controlled gas sorption in porous coordination frameworks. *Nature Communications* **9**, doi:10.1038/s41467-018-06850-6 (2018).
- 259 Gong, X. Y. *et al.* Insights into the Structure and Dynamics of Metal-Organic Frameworks via Transmission Electron Microscopy. *Journal of the American Chemical Society* **142**, 17224-17235, doi:10.1021/jacs.0c08773 (2020).
- 260 Hosono, N., Terashima, A., Kusaka, S., Matsuda, R. & Kitagawa, S. Highly responsive nature of porous coordination polymer surfaces imaged by in situ atomic force microscopy. *Nature Chemistry* **11**, 109-116, doi:10.1038/s41557-018-0170-0 (2019).
- 261 Parent, L. R. *et al.* Pore Breathing of Metal-Organic Frameworks by Environmental Transmission Electron Microscopy. *Journal of the American Chemical Society* **139**, 13973-13976, doi:10.1021/jacs.7b06585 (2017).
- 262 Soldatov, M. A. *et al.* The insights from X-ray absorption spectroscopy into the local atomic structure and chemical bonding of Metal-organic frameworks. *Polyhedron* **155**, 232-253, doi:10.1016/j.poly.2018.08.004 (2018).
- 263 Bordiga, S., Bonino, F., Lillerud, K. P. & Lamberti, C. X-ray absorption spectroscopies: useful tools to understand metallorganic frameworks structure and reactivity. *Chemical Society Reviews* **39**, 4885-4927, doi:10.1039/c0cs00082e (2010).
- 264 Kortright, J. B., Marti, A. M., Culp, J. T., Venna, S. & Hopkinson, D. Active Response of Six-Coordinate Cu²⁺ on CO₂ Uptake in Cu(dpa)₂SiF₆-i from in Situ X-ray Absorption Spectroscopy. *Journal of Physical Chemistry C* **121**, 11519-11523, doi:10.1021/acs.jpcc.7b02623 (2017).
- 265 Bon, V. *et al.* Exceptional adsorption-induced cluster and network deformation in the flexible metal-organic framework DUT-8(Ni) observed by in situ X-ray diffraction and EXAFS. *Physical Chemistry Chemical Physics* **17**, 17471-17479, doi:10.1039/c5cp02180d (2015).
- 266 Neu, J. & Schmuttenmaer, C. A. Tutorial: An introduction to terahertz time domain spectroscopy (THz-TDS). *Journal of Applied Physics* **124**, doi:10.1063/1.5047659 (2018).
- 267 Withayachumnankul, W. & Naftaly, M. Fundamentals of Measurement in Terahertz Time-Domain Spectroscopy. *Journal of Infrared Millimeter and Terahertz Waves* **35**, 610-637, doi:10.1007/s10762-013-0042-z (2014).
- 268 Neu, J. *et al.* in *2019 44th International Conference on Infrared, Millimeter, and Terahertz Waves (IRMMW-THz)*. 1-2.
- 269 Kamencek, T., Bedoya-Martinez, N. & Zojer, E. Understanding phonon properties in isorecticular metal-organic frameworks from first principles. *Physical Review Materials* **3**, doi:10.1103/PhysRevMaterials.3.116003 (2019).
- 270 Formalik, F., Fischer, M., Rogacka, J., Firlej, L. & Kuchta, B. Effect of low frequency phonons on structural properties of ZIFs with SOD topology. *Microporous and Mesoporous Materials* **304**, doi:10.1016/j.micromeso.2018.09.033 (2020).
- 271 Itakura, T. *et al.* The role of lattice vibration in the terahertz region for proton conduction in 2D metal-organic frameworks. *Chemical Science* **11**, 1538-1541, doi:10.1039/c9sc05757a (2020).
- 272 Ryder, M. R. *et al.* Identifying the Role of Terahertz Vibrations in Metal-Organic Frameworks: From Gate-Opening Phenomenon to Shear-Driven Structural Destabilization. *Physical Review Letters* **113**, doi:10.1103/PhysRevLett.113.215502 (2014).
- 273 Hoffman, A. E. J., Wieme, J., Rogge, S. M. J., Vanduyfhuys, L. & Van Speybroeck, V. The impact of lattice vibrations on the macroscopic breathing behavior of MIL-53(Al). *Zeitschrift Fur Kristallographie-Crystalline Materials* **234**, 529-545, doi:10.1515/zkri-2018-2154 (2019).
- 274 Tan, N. Y. *et al.* Investigation of the terahertz vibrational modes of ZIF-8 and ZIF-90 with terahertz time-domain spectroscopy. *Chemical Communications* **51**, 16037-16040, doi:10.1039/c5cc06455d (2015).

- 275 Ryder, M. R., Civalleri, B., Cinque, G. & Tan, J. C. Discovering connections between terahertz vibrations and elasticity underpinning the collective dynamics of the HKUST-1 metal-organic framework. *Crystengcomm* **18**, 4303-4312, doi:10.1039/c5ce02347e (2016).
- 276 Ryder, M. R. *et al.* Detecting Molecular Rotational Dynamics Complementing the Low-Frequency Terahertz Vibrations in a Zirconium-Based Metal-Organic Framework. *Physical Review Letters* **118**, doi:10.1103/PhysRevLett.118.255502 (2017).
- 277 Zhang, W. *et al.* Probing the Mechanochemistry of Metal-Organic Frameworks with Low-Frequency Vibrational Spectroscopy. *Journal of Physical Chemistry C* **122**, 27442-27450, doi:10.1021/acs.jpcc.8b08334 (2018).
- 278 Brammer, L. *et al.* Advanced characterisation techniques: multi-scale, in situ, and time-resolved: general discussion. *Faraday Discussions* **225**, 152-167, doi:10.1039/D0FD90032J (2021).
- 279 Fraux, G., Chibani, S. & Coudert, F. X. Modelling of framework materials at multiple scales: current practices and open questions. *Philosophical Transactions of the Royal Society a-Mathematical Physical and Engineering Sciences* **377**, doi:10.1098/rsta.2018.0220 (2019).
- 280 Chong, S., Lee, S., Kim, B. & Kim, J. Applications of machine learning in metal-organic frameworks. *Coordination Chemistry Reviews* **423**, doi:10.1016/j.ccr.2020.213487 (2020).
- 281 Chibani, S. & Coudert, F. X. Machine learning approaches for the prediction of materials properties. *Appl Materials* **8**, doi:10.1063/5.0018384 (2020).
- 282 Marques, M. A. L. & Gross, E. K. U. Time-dependent density functional theory. *Annual Review of Physical Chemistry* **55**, 427-455, doi:10.1146/annurev.physchem.55.091602.094449 (2004).
- 283 Khan, I. M., Alam, K. & Alam, M. J. Exploring charge transfer dynamics and photocatalytic behavior of designed donor-acceptor complex: Characterization, spectrophotometric and theoretical studies (DFT/TD-DFT). *Journal of Molecular Liquids* **310**, doi:10.1016/j.molliq.2020.113213 (2020).
- 284 Van Speybroeck, V., Vandenhoute, S., Hoffman, A. E. J. & Rogge, S. M. J. Towards modeling spatiotemporal processes in metal-organic frameworks. *Trends in Chemistry* **3**, 605-619, doi:<https://doi.org/10.1016/j.trechm.2021.04.003> (2021).
- 285 Kumar, N., Weckhuysen, B. M., Wain, A. J. & Pollard, A. J. Nanoscale chemical imaging using tip-enhanced Raman spectroscopy. *Nature Protocols* **14**, 1169-1193, doi:10.1038/s41596-019-0132-z (2019).